Origin and Preservation Conditions of Organic Matter in the Mozambique Channel: Evidence for Widespread Oxidation Processes in the Deep-Water Domains

Torelli Martina [1, *], Battani Anne [1], Pillot Daniel [1], Kohler Eric [1], De Azevedo Joel Lopes [1], Kowalewski Isabelle [1], Pastor Lucie [2], Brandily Christophe [2], Schmidt Sabine [3], Jouet Gwenael [4], Deville Eric [1]

[1] IFP Energies Nouvelles, 1-4 Av. de Bois-Préau, 92852, Rueil-Malmaison Cedex, France
[2] IFREMER, Centre, de Bretagne, REM/EEP, Laboratoire Environnement Profond, F-29280 Plouzané, France
[3] UMR5805 EPOC, CNRS, OASU, Université de Bordeaux, 33615 Pessac, France
[4] IFREMER, Centre, de Bretagne, REM/GM, Laboratoire Cycles Géochimiques et ressources, F-29280 Plouzané, France

* Corresponding author : Martina Torelli, email address : torellimartina.90@gmail.com

Abstract :

The Mozambique and Madagascar margins present major rivers that are responsible for the discharge of large amounts of terrestrial organic matter (OM) which can influence carbon cycling in marine environments. Therefore, the Mozambique channel represents a unique case to study the fate of the organic carbon in deep-water domains. Using a new and extensive data set of sedimentary OM collected from sediment traps, seafloor sediments and core sediments, we address the origin of the OM that is transported and deposited in the Mozambique Channel, its degradation state and preservation conditions. A Rock-Eval 6 survey allowed us to characterize the origin and amount of OM from shallow to deep-water turbidite systems, between 500 and 4400 m water depth. Rock-Eval 6 performed on suspended sediments within particle traps at 47 m above the seabed show that the OM is transported into the deep-water domain with relatively high TOC (between 1.5 and 2.5%). However, the OM is largely oxidized close to the water-sediment interface (Oxygen Index >300 mg CO2/g TOC). Seafloor sediments sampled to a maximum depth of 40 cm show lower TOC values compared to those collected from particle traps suggesting that the degradation of the OM is mainly active at the water-sediment interface. Small concentrations of OM are preserved within the recent sediments of the distal area of the Zambezi turbidite system below 2500 m water depth (TOC < 0.5%). Rock-Eval results show that core sediments from the Majunga slope (NW margin of Madagascar) and the Zambezi slope (Mozambique margin) contain the highest concentration of terrestrial OM (TOC between 1 and 2%). However, the OM within core sediments from the deep-water domain is largely oxidized and degraded, probably due to the conjugate effect of low sediment accumulation rates (SAR) and high permeabilities of the coarse-grained sediments. Consequently, the deep-water domain of the Mozambique Channel does not seem to be an important sink of terrestrial OM. This process is reinforced by important bottom water currents which induce the remobilization and transport of seafloor sediments that lead to higher oxygen exposure time in the uppermost centimeters of sediments.

Highlights

► Origin and deposition of the Organic Matter in the main physiographic provinces of the Mozambique Channel ► Rock-Eval 6 data and $\delta^{13}C$ isotopic signature to determine the variability of OM composition within suspended, seafloor and core sediments ► EDS-SEM analysis, Sediment Accumulation Rates and Oxygen Exposure Times to assess the preservation condition of the OM in the Mozambique Channel ► Important bottom currents are prone to maintain higher OET by the remobilization of the uppermost sediments and its OM ► Small concentration of terrestrial OC (TOC < 0.5%) are preserved in seafloor sediments of deep-water domain

1. Introduction

More than 80% of the particulate Organic Matter (OM) is buried on continental and insular margins (Hedges and Keil, 1995). The burial rate of OM in marine settings affects the sediment Organic Carbon (OC) budget (Burdige 2007) which is still not well understood and remains questionable (Gordon and Goñi 2003). It is well known that the burial of OC in marine sediments is a sink for CO_2, possibly greater than that resulting from the alteration of silicates (Gailladert et al. 1999; Galy et al., 2015). Therefore, quantifications of lateral fluxes of OC from land to oceans are key controlling factor for CO_2 exchange with the atmosphere and the natural carbon cycle (Regnier et al. 2013). In addition, transport conditions of OC to oceans on the geological time scale determine whether it may be a source or sink to the active carbon cycle (Bröder et al. 2018).

OC is transported mainly by rivers to the ocean, with a flux estimated between 410 TgC.y^{-1} and 580 TgC.y^{-1} (Schlesinger and Melack, 1981; Romankevich et al. 2009; Mignard et al. 2017). Most of the OM entering continental shelf areas is rapidly re-mineralized (Hedges 1997; Burdige 2005) but a fraction of it can be preserved and eventually reaches deep-water domains (Baudin et al. 2020; Mignard et al. 2017). The efficiency of such a process is controlled by the type of OM (*e.g.* terrestrial or "type III" *vs* marine or "type II") which can lead to selective degradation and preservation conditions (Hedges et al. 1988; Stow 2001, Burdige 2007). It is well known that terrestrial OM which is composed mainly of higher plant residues, is more resistant to degradation than marine OM which derives from marine phytoplankton (Cowie et al. 1992; Burdige 2007). Therefore, higher amounts of terrestrial OM are more likely to migrate from the shelf to the deep-water domains, mainly transported by lateral movement of the sediments (*e.g.* turbidites). In contrast, marine OM is generally dominated by vertical movement of particles (*e.g.* Mollenhauer et al. 2007). In addition to the lability of the OM, there are several factors that control its preservation before and after sedimentation along the continental shelf such as (a) primary productivity and rate of OM supply (Pedersen and Calvert 1990; Jahnke 1990), (b) oxygen conditions of the water column and in the uppermost centimeters of sediments (Hartnett et al. 1998), (c) sedimentation rate (Muller and Suess 1979, Burdige 2007) and, (d) grain size (Keil et al. 1994).

Conventional hypotheses concerning OM preservation did not consider scenarios with large accumulations of OM in deep-water areas (Suess 1980). However, deep-water depositional

environments can be characterized by important OM accumulations, as observed by Stow et al. (2001) in the Makkassar Strait (Indonesia). The terrestrial OM found in Quaternary sediments is transported through the Mahakam Delta Province by turbidity currents, and deposited at more than 2000 m of water depth with relatively high Total Organic Carbon (TOC) content (between 1% and 2%) (Stow et al. 2001). Another example of such depositional environment is the Congo system in which the terrestrial OM is transported 760 km offshore through the canyon to the distal fan (Vangriesheim et al., 2009; Baudin et al., 2010; Baudin et al., 2017). Within the distal lobes, TOC values range from 3.5% to 4% (Baudin et al. 2017) due to an efficient OM preservation process. Also there is a direct connection between canyon and river. Therefore, the deep-water domain of the Congo system is a great sink of continental OC (Baudin et al. 2017). Maier et al. (2019) discussed the fate of the OC reaching the deep-water domain along the Monterey Canyon (offshore California) at water depths between 278 and 1849 m, based on the analysis of OM collected in sediment traps and sediment cores. According to the isotopic signature of OC from sediment traps, the water column is more enriched in marine OM than sediments at the sea floor that show a higher terrestrial contribution. The marine OM is better preserved in the water column, as the effect of sediment transport in the canyon induces deposition and reworking of seafloor sediments which results in a higher consumption and degradation of the marine OM compared to the terrestrial ones (Maier et al. 2019).

Knowing that, we propose to study the origin, fate and preservation state of OM in the turbiditic system of the Mozambique Channel to assess whether this area acts as a sink of carbon as the other systems cited above. This system provides a unique opportunity to study the OC in the deep-water domains where major rivers (Fig. 1) are responsible for the discharge of large amounts of terrestrial OM. We propose a new approach that studies the distribution of the OM along the entire channel from within the water column to the very early deposition, using sediment traps, interface cores and piston sediment cores. We combine Rock-Eval data, elemental analyses of carbon and $\delta^{13}C$ values to assess the origin and degradation-preservation processes during deposition, from shallow to deep-water turbidite systems (between 500 and 4400 m of water depth). Using additional data of sediment accumulation rates and oxygen micro-profiles, the evolution of the recently deposited OM is compared between the main physiographic provinces of the Mozambique Channel. Finally, a sample from each margin was analyzed using Energy Dispersive X-Ray Spectroscopy – Scanning Electron Microscopy (EDS-SEM) to identify the nature of the mineralogical

4

composition and the lithofacies of the sediments which has an important impact on OM preservation.

2. Geological framework

The Mozambique channel corresponds to a wide straight between Africa and Madagascar (Fig. 1). It was formed progressively, during more than 140 Ma, since the breakup of Gondwana (Rabinowitz et al., 1983) and the formation of the oceanic lithosphere of the Mozambique Basin during Jurassic-Cretaceous times (Mueller and Jokat, 2019; Thompson et al., 2019). The central part of the Mozambique Channel is still tectonically active today as the southern prolongation of the eastern branch of East African Rift System, and this tectonic activity has controlled the development of volcanic systems and related seamounts emerging locally in Europa and Bassas da India (Deville et al., 2018). This active tectonic setting is also associated with a zone of uplift which has influenced the sedimentary pattern, notably the Zambezi turbidite system (Fierens et al., 2019). The continental margins of the Mozambique Channel are mostly steep transform or transtensive margins.

The Mozambique Basin is largely filled by a turbidite system from the Zambezi River, the main river along the east African coast. It is also partly filled by turbidite currents from Madagascar, mainly focused in the Tsiribihina submarine valley which is sourced mainly by the Tsiribihina and Mangoki Rivers (Fierens et al., 2019; Fig. 1). The Betsiboka and Mahavavy Rivers, in the north-western part of Madagascar, are responsible for large sedimentary accumulations on the continental shelf (Berthois and Crosnier, 1966; Wiles et al., 2009; Pastor et al., 2020; Fig. 1). These rivers coming either from Africa or Madagascar provide large detrital OM input to the Mozambique Channel.

In the Mozambique Basin, strong bottom currents have been described even in the very deep-water areas (between 2000 and 4000 m water depth) (Miramontes et al., 2019). These bottom currents are responsible for the development of eddies which partly block the Mozambique undercurrents, enhancing southward flow along the Zambezi Channel. Measured bottom currents in the Zambezi and Tsiribihina submarine valleys reach more than $50\,\mathrm{cm.s}^{-1}$, and these strong bottom currents are responsible for strong erosion processes along the Zambezi deep sea valley (Miramontes et al., 2019).

3. Material and methods

This study was conducted in the framework of the PAMELA (PAssive Margin Exploration LAboratory) research project (Bourillet et al., 2013) which included several oceanographic exploration surveys in the Mozambique Channel, Pamela-Moz01 (Olu, 2014), Pamela-Moz04 (Jouet and Deville, 2015) and Pamela-Moz08 (Khripounoff, 2016). Samples were collected along the Zambezi system (slope, valley and distal part) and Tsiribihina turbidite systems, as well as along the continental slope off the Betsiboka and South-Mahavavy Rivers (the largest rivers of NW Madagascar) (Fig. 1). The main objective of this sampling campaign was to gain an understanding of the evolution of the OM in Quaternary sediments along the eastern margin of Africa.

Sediment traps in moorings located 47 m above the seabed are described in Miramontes et al. (2019) and Pastor et al (2020). We will refer to such samples as "suspended sediments". Recovered suspended sediments were kept at 4°C for treatment in the laboratory. Interface cores were collected with an interface multicorer (MTB, 30-40 cm maximum penetration), referred as "seafloor sediments". These cores were sliced vertically on-board and samples were kept frozen (-20°C) to be analyzed in the laboratory. Piston sediment cores were collected with the Küllenberg corer (KS or KSF, recovered core length up to 12 m) of the R/V *Atalante* (Pamela-Moz01 survey) and the Calypso corer (CS or CSF, recovered core length up to 33 m) of the R/V *Pourquoi Pas?* (Pamela-Moz04 survey). We will refer to such samples as "core sediments". Samples were taken on-board and kept at 4°C to be analyzed in the laboratory. Sampling systems with sediment traps, interface cores and gravity/piston cores are described in Supplementary Material (Fig. S1, Appendix A).

3.1 Rock-Eval

Rock-Eval pyrolysis is a standard method for the study of organic-rich rocks. The method was originally developed for petroleum applications as it provides a rapid determination of the content, type and maturity of organic matter (Espitalié et al., 1977, 1984; Lafargue et al., 1998; Behar et al., 2001). In addition, Rock-Eval also yields information about type and amount of carbonates within sedimentary rocks (Pillot et al., 2014). Rock-Eval analysis can be performed either on the bulk rock (Espitalie et al., 1977) or on concentrated organic matter samples (Behar et al., 2001). Rock-Eval 6 analysis (Lafargue et al., 1998) consists of pyrolysis during which samples are heated first in a pyrolysis furnace under inert gas, and

7

then in a combustion furnace using air which allows to determine the petroleum potential of a sedimentary rock. The hydrocarbons liberated during the progressive heating are measured with an FID (Flame Ionization Detector) and form the peak S1 that represents the free thermo-vaporized hydrocarbons. The peak S2 corresponds to the liquid effluents released during cracking of organic matter. The residual sediments are then subjected to a progressive combustion (oxidation under air). CO and CO_2 are released during pyrolysis and combustion and are measured continuously using Infra-Red cells. The peak S3 corresponds to the CO_2 content released during pyrolysis of the insoluble organic matter (kerogen). These measurements quantify the inorganic carbon ($_{MIN}C$) and the TOC of the analyzed samples. The amount of bulk rock required for Rock-Eval analysis ranges from 50 to 70 mg. In this study, we applied a method used at IFP Énergies Nouvelles (IFPEN) adapted for recent sediments (Deroo et al., 1983; Deville et al., 2015) which applies a lower heating program than used normally for the study of consolidated sediments, with an initial plateau of 200°C (procedure adapted for immature sediments) instead of 300°C. In addition, samples were first rinsed with fresh water because they were poorly compacted and rich in seawater. Samples were then centrifuged and dried prior to the analysis. These preparation steps were carried out to overcome problems related to the presence of sodium chloride which can generate HCl and induce an early destabilization of carbonates during pyrolysis and subsequent damage to the analyzing device. A similar method has also been used by Baudin et al. (2017). Rock-Eval Total Carbon (TC%) values of all core samples have been cross-checked with TC (%) values obtained by elemental analyses (Fig. 2A). Also, calcite content (%) obtained with Rock-Eval (Pillot et al., 2015) has been compared with XRF (X-Ray Fluorescence) data using the XRF Avaatech scanner (Fig. 2B).

3.2 OC content and $\delta^{13}C$ of sedimentary organic carbon

For specific seafloor sediments (MOZ4-MTB4 and MTB5, and MOZ1-MTB10, MTB12 and MTB15), Total Carbon (TC %) content was determined using a Leco CNS-2000 auto-analyzer using acetanilide for calibration. The relative standard deviation (RSD) was typically < 3% on samples duplicates. Carbonates were removed with HNO_3 (30%) at a constant temperature of 60°C overnight. Subsequently, OC (%) content was determined using the Leco CS-125 elemental analyzer using steel chips from LECO for the calibration. The RSD of the measurement was <1% based on 17 standards replicates and typically < 5% on samples duplicates. Differences between TC (%) and OC (%) allowed to determine the Inorganic Carbon ($_{MIN}C$) content (%) (Pastor et al. 2020).

Isotopic signature of the sedimentary organic carbon (δ^{13}C) for 52 samples from specific sediment traps (*i.e.* MLP 3, MLP5, MLP7, MLP8) was assessed through the Combustion Module-Cavity Ring Down Spectroscopy (CM-CRDS - Picarro) (Balslev-Clausen et al., 2013). Samples were acidified with HCl 1 N at 40 °C until carbonates were completely dissolved. Samples were rinsed again using milli-Q water to remove acid residues. After a freeze-drying process, around 10 mg were then analyzed in a small capsule of 5×9 mm. Calibration was performed according to the International Atomic Energy Agency (IAEA) reference material (Pastor et al. 2020). Precision was typically within 0.03‰ for a triplicate.

3.3 EDS-SEM analysis

EDS-SEM techniques are used to determine the microscopic structure of minerals and organic matter assemblages producing a surface map of the chemical composition of the sample. The sample is then converted into a mineralogical map of the total matrix. We present here EDS-SEM results from two samples that are not consolidated and characterized by very low permeability. The first sample was collected along the Zambezi continental slope at 78 cm bsf from the top of core MOZ04-CS17 (602 m of water depth). The second sample is from the Majunga continental slope at 54 cm bsf from the top of the core MOZ01-KSF12 (735 m of water depth). Samples were first dried 1 week at 60°C and subsequently frozen at -80°C and then lyophilized. Lyophilization is a process that removes the water from low permeability material with limited damage to the micro-structure of the sample. Because of their low permeability, samples have been impregnated with a depressurization cup at − 0.8 bar to enable injection of the resin in the small sample pores. The impregnated samples were then sawed and polished for the SEM analysis. Microscopy was performed with a "high vacuum" conventional SEM (EVO MA10, Zeiss SMT) in IFPEN laboratories. A motorized five axis stage provided a first visualization of the samples. The electron microscope is equipped with a tungsten filament at 15 kV and 100 mA and uses a probe current at 700 to 750 pA for EDS analysis (mineral identification). It is also used with a probe current at 150 pA for secondary electron (SE) imaging at high spatial resolution to observe the surface topography, and with a back scattered electron detector (BSE) to obtain images with atomic number contrast. The calibration of the silicon drift detector of EDS is done on pure cobalt for quantitative analysis during 10 s at 10 to 15 kcps (kilo-counts per second), with a dead time of about 15%. In some cases, XRD is not sufficient to identify minerals. In this case, SEM micrography coupled with EDS analysis can be used to identify and define mineral phases through their chemical composition. Chemical micro-analysis is standardized on various minerals with a well-known

chemical composition and controlled by electron microprobe (Reference standards for X-ray microanalysis n° 7610 from Micro-Analysis Consultant Limited, UK).

3.4 Sediment accumulation rates

Sediment accumulation rates (SARs) are determined with different methods depending on the available samples. SARs were calculated from depth profiles of excess ^{210}Pb (^{210}Pb$_{xs}$; $T_{1/2}$ = 22.3 years) of interface cores from the Madagascar and Mozambique Margins: MOZ1-MTB6 (Fontanier et al., 2018), MOZ1-MTB3, MOZ4-MTB2 and MOZ4-MTB3 (Pastor et al., 2020) and MOZ4-MTB4 and MOZ4-MTB5 (this work). Activities of ^{210}Pb and ^{226}Ra were determined on sediment samples by gamma spectrometry using a well-type, high-efficiency gamma detector "Canberra" (Schmidt and De Deckker, 2015). The detector was calibrated using IAEA reference material. Activities are expressed in mBq g^{-1} and errors are based on one standard deviation counting statistics. Excess ^{210}Pb was calculated by subtracting the activity supported by its parent isotope, ^{226}Ra from the total ^{210}Pb activity in the sediment. Sediment layers were measured downcore until reaching negligible excess values. Mean SARs were calculated from the ^{210}Pb$_{xs}$ profiles assuming constant flux and constant sedimentation (referred to as the CF:CS model). SAR along the Zambezi deep sea valley has been deduced from a single radiocarbon dating performed on foraminifera on the interface core MOZ1-MTB10 at 35 cm below seafloor. As seafloor sediments were not available in the Tsiribihina valley, a minimum SAR was estimated by converting the mean annual mass flux measured by a moored sediment trap placed 47 m above the sea floor over a period of 13 months (Miramontes et al., 2019) and assuming a density of 1.5 g cm^{-3} (average gamma density measured on piston cores).

3.5 O$_2$ microprofiling

The O$_2$ profiles were measured on interface cores kept in a refrigerated box to reproduce a temperature close to the *in-situ* conditions. For each station, the oxygen concentration in the bottom water was determined by the Winkler titration technique adapted by Aminot and Kérouel (2004). The surface water was gently bubbled to avoid any stratification during the profiling. A microsensor multimeter (Unisense S/A, Denmark) with one to two Clark type oxygen probes Ox-50 (Revsbech, 1989) with a motor controller were used to record depth microprofiles inside the sediment with a 50 to 500 μm resolution depending on the oxygen penetration depth. A linear calibration was performed between the oxygen concentration measured in the overlying water and an oxygen free solution. Between 1 and 12 profiles were

performed on each core. For each profile, the oxygen penetration depth (OPD) was estimated. *In situ* oxygen exposure times (OET) were calculated as the ratio between OPD and SAR (Hedges and Keil, 1995, Pastor et al. 2011). OET provide an estimate of the time during which accumulating uppermost sediments are exposed to molecular oxygen. However, sediments are likely impacted by lateral OET as function of the sediment transport time which represent a controlling parameter on OM degradation across continental shelfs (Keil et al. 2004; Bröder et al. 2018). A few estimates of lateral OET give a broad range of impact on overall OET: Bröder et al (2018) concluded that the lateral OET is order of magnitude higher than the *in-situ* in Siberian-Artic land ocean while Keil et al., (2004) concluded that lateral OET could double the overall OET along the Washington margin. Hence, lateral OET are intimately dependent on regional settings. In this study, transport of OM is mainly driven by turbidity currents, which can transport a particle several hundreds of km away in few years as showed in the Congo system (Rabouille et al. 2009). Given that and the high calculated *in situ* OET in the distal area, we assume that lateral OET contribution is negligible compared to *in situ* OET.

4. Results

The characterization of the OM degradation-preservation processes from shallow to deep-water turbidite systems of the Mozambique Channel is mainly based on Rock-Eval 6 (RE6) analyses of core sediments, seafloor sediments and suspended sediments. Full results are attached in Supplementary Material (Table S1, Appendix B). Here, RE6 results are presented as average values by piston core, interface core and sediment trap (Table 1). The location of the sampling sites is presented in Figure 1 and detailed locations are indicated in Table 1.

The TC (%) content obtained by RE6 and Leco shows a good correlation (R^2= 0.9; Fig. 2A). Also, $CaCO_3$ content determined from RE6 and Ca content determined from XRF show the same vertical trend (Fig. 2B). Note that samples presented in Figure 2 were selected from the same levels, but the analysed material is not exactly the same which explains the small differences. Therefore, the comparison of (1) TC measured by Rock-Eval method with Leco, and (2) Inorganic Carbon ($_{MIN}C$) measured with XRF demonstrates that the TOC determined from Rock-Eval is reliable and can be considered calibrated for this study.

For suspended sediments, $\delta^{13}C$ analysis of OC, in addition to other proxies like RE6 measurements, could help to better assess OM origin. $\delta^{13}C$ values in the range between -17 ‰ and -23 ‰ are typical for marine phytoplankton, -24 ‰ to – 30 ‰ for C3 plants (typically mangroves) (Bouillon et al., 2008), and -8 and -15 ‰ for C4 plants (Yeh and Wang 2001). Therefore, the measured $\delta^{13}C$ in this study, which are slightly lighter than -21 ‰, can be considered either as a marine contribution or a mix between sources.

4.1 Analyses of suspended sediments

Particles collected by moored sediment traps located at 47 m above the seabed show TOC values between 1.5% and 3.5%, S2 peaks between 2.3 and 10 mg HC/g of rock (Fig. 3a), HI values between 180 and 300 mg HC/g TOC, and OI values between 150 and 300 mg CO_2/g TOC (Fig. 3b). Considering a reference HI value of 400 mg HC/g TOC and 100 mg HC/g TOC for marine and terrestrial OM respectively (Espitalie et al., 1985), we can assume that the OM analyzed from particle traps is mainly terrestrial (Table 1). Rock-Eval results seem to be confirmed by the $\delta^{13}C$ values of OC from suspended sediments which vary between -21.5 and -22.1 ‰ (Table 2; Fig. 4). These results suggest that continental-derived OM is transiting along continental slopes, and is transported down to the distal area of the Zambezi turbidite

system, thereby preserving high TOC and HI values (Fig. 3). However, the isotopic signature can also indicate a mixture of marine and terrestrial OM, with a higher input of terrestrial material. Note that suspended sediments from the distal valley show S2, TOC, HI and OI values similar to the suspended sediments collected in the Tsiribihina submarine valley or even in the Majunga margin, rather than the Zambezi valley (Fig. 3b; Table S1).

4.2 Analyses of seafloor sediments

Results obtained from seafloor sediment samples at a maximum depth of 30 – 40 cm (MTB) show lower values in TOC (0.6 to 1.43%), S2 (2.5 to 10 mg HC/g rock), and HI (180 to 320 mg HC/ g TOC) as compared to suspended sediments (Table 1). OI values are lower than 300 mg CO_2/g TOC in the Majunga area, in the Tsiribihina channel area and in the distal channel of the Zambezi turbidite system and up to 600 mg CO_2/g TOC along the Zambezi slope (Table 1 and Supplementary material, Table S1, Appendix B). T_{max} values are relatively high for this completely immature OM which can be interpreted as an advanced state of OM degradation of humic substances (Hare et al., 2014). Rock-Eval analysis on seafloor sediments were performed on two samples collected at a specific depth interval for each MTB (0.5 cm and 6.5 cm) (Table S1). TOC value strongly decreases in seafloor sediments located in the distal depositional areas (Fig. 1, Table S1). Therefore, additional analyses through Leco were performed on 65 samples from specific MTBs (MOZ1-MTB10, MOZ1-MTB12, MOZ1-MTB15) (Fig. 1) to better determine their OC (%) content (Fig. 5). They yield very low OC (%) content between 0.2 to 0.5 %. Suspended sediments in the same distal regions show higher TOC values (between 1.5% to 2.6%) (Table 1; Fig. 3) suggesting that the OM is transiting to the deep-water domains while minimally affected by degradation. However, the OM is rapidly degraded once it is deposited (Fig. 5).

4.3 Analysis of core sediments

Core sediments in the Mozambique Channel have been collected at a maximum depth from 12 to 33 m. They show moderate TOC (TOC < 1.8%), S2 (< 2 mg HC/g of rock) and T_{max} values characteristic of immature sediments (< 420°C) (Table 1). A higher OM content is observed in the northwestern part of Madagascar (Majunga margin), where the slope is fed by major rivers such as Betsiboka and South-Mahavavy. Higher OM content is also observed in the Davie Ridge area and along the Zambezi continental slope (Fig. 6). All samples show a low HI of around 300 mg HC/g TOC and a higher OI, with a mean value of 300 mg CO_2/g TOC (Table 1). Note that HI and OI values are not given for TOC values < 0.5% because they

are considered not reliable. These results are characteristic of a terrestrial OM composed mainly of higher plants (type III) (van Krevelen, 1950). However, we do observe differences in terms of HI for samples from the Majunga and the Davie Ridge sectors compared to the Zambezi slope (Fig. 6). Samples show a first trend of HI values between 50 and 100 mg HC/g TOC, with a mean value of 75 mg HC/g TOC. A second trend is characterized by a mean HI value of 150 mg HC/g TOC. Therefore, differences in terms of HI may be related to different oxidation conditions of the initial terrestrial OM, or to a mixture of marine and terrestrial OM. Sediments from the Zambezi continental slope contain type III OM, with S2 values around 1 mg HC/g rock and a TOC content of up to 1.8%. Sediments collected from the Zambezi turbidite system, both from the valley and from the distal depositional area, are characterized by low S2 values < 0.5 mg HC/g rock and TOC < 0.8% (Fig. 6). Sediments from the Tsiribihina turbidite system (sourced from Madagascar) show even lower TOC values between 0.13 and 0.61%. Finally, samples collected in the distal area of the Mozambique basin show the lowest S2 (< 0.3 mg HC/g rock) and TOC values (< 0.2%; Fig.6). As such, a strong OM decrease is observed with increasing water depth, from the Zambezi continental slope to the distal valley of the Zambezi turbidite system (Fig. 7).

According to RE6, following the method of Pillot et al. (2014) which allows us to characterize and quantify carbonates in solid samples, mineral carbon is present in all samples, mainly in the form of calcium carbonate. Fig. 8 and Fig. 9 show the content of organic carbon (TOC %) and inorganic carbon ($_{MIN}$C %) in the analyzed core samples as a function of depth. Depending on the core location, the OM content is either correlated (CS17, CS21, CS25, CS26) or anti-correlated (CS22, Fig. 9) with the mineral carbon content. In the latter case, the dilution of the OM is related to an increase of carbonate-rich turbidites that are sourced from Bassas da India Island (Fig. 1).

4.4 EDS-SEM analyses on core sediments

EDS-SEM analyses have shown that core sediments from the Zambezi continental slope and in the Majunga margin (respectively samples MOZ04-CS17-S1-78 and MOZ01-KSF12-S1-54) are mainly characterized by a matrix composed of very fine sediments and shell debris principally made of calcite, with a mean size of 100 μm dispersed in the matrix (Fig. 10; Table 3). All samples show quartz, calcite and feldspar, and minerals are usually well preserved and not altered. However, a drastic textural difference appears between the sediments collected from the Zambezi slope and those from the Majunga slope. The samples

14

from the Majunga slope show a better preservation compared to those from the Zambezi slope which appears largely damaged (Fig. 10). The composition and quantities of chemical elements are very different between these two areas (Table 3). EDS-SEM shows that CS17-S1-78 is composed mainly of K-feldspar and phyllosilicates such as mica (biotite and muscovite; Fig. 11). Aggregates of iron oxides are found inside marine bioclasts and inside OM which is also partly calcified, with accumulation of silica (Fig. 12). The MOZ01-KSF12-S1-54 sample (offshore Majunga) is composed mainly of calcite and aragonite, with small amounts of K-feldspar and mica. These sediments are very rich in bioclasts but they do not show accumulation of iron oxides (Fig. 13) which is in contrast with measurements presented by Pastor et al. (2020) showing that iron oxides are abundant.

4.5 Sediment accumulation rates

^{210}Pb-derived SARs range from 0.4 to 2.49 cm yr^{-1} in the Madagascar margin (Fontanier et al., 2018; Pastor et al., 2020) and from 0.064 to 1.43 cm yr^{-1} in the Mozambique margin (this study; Table 4; Fig. S2, Appendix A). In the Zambezi channel, radiocarbon dating gave a calibrated age of 7090 ± 150 Cal yrs BP (calibrated years before the present) (6580 ± 30 ^{14}C yrs BP) and thus a minimum SAR of approximately 0.005 cm yr^{-1} (Table 4). In the Tsiribihina valley, mass accumulation rates in a sediment trap gave a value of 8 mg cm^{-2} yr^{-1}. This is equivalent to a sediment accumulation rate of 0.012 cm yr^{-1} (assuming a density of 1.5 g cm^{-3} for the sediments; Table 4). Note that this SAR value is a minimum estimate because it does not integrate the sediment supply which occurs laterally between the sediment traps (47 m above seabed) and the seabed, notably coarse clastic material transported by turbidite/contourite currents.

4.6 Oxygen penetration depths

At most sites of the study area, oxygen concentration disappears within the upper 3 cm of sediment, except in the Tsiribihina (MOZ1-MTB12) and Zambezi valleys (MOZ1-MTB10 and MOZ1-MTB15; Fig. 14) of the deep-water area of the Mozambique Channel. The lowest measured oxygen penetration depth (OPD) gave a value of 5 mm (Table 4). They were found in the Madagascar margin in reduced sediments that were affected by methane diffusion (MOZ4-MTB1 and MOZ4-MTB3; Pastor et al., 2020). The highest OPD were found in the Tsiribihina (> 9 cm at MOZ1-MTB12) and Zambezi valleys (8.3 cm at MOZ1-MTB10; > 9 cm at MOZ1-MTB15). At the greatest depth which is in the distal part of Zambezi valley (4070 m at MOZ1-MTB15), concentrations were still above 25 μM at 8 cm (Fig. 14).

15

Assuming a continual decrease in oxygen concentration with depth, the OPD in the Tsiribihina valley and the Zambezi distal channel can be estimated to 11 and 12 cm respectively (Table 4). OET values are low in the margins (less than 200 years) whereas they reach several thousands of years in the deep-water area of the Mozambique basin (Table 4).

5. Discussion

5.1 Origin of the sedimentary OM

It is generally assumed that carbon flux decreases with water depth due to degradation of OM within the water column (Suess, 1980). Yet this process holds more for the marine OM flux (type II) compared to the continental OM flux (type III). Several studies have shown that terrestrial OM can be transported by down-slope movements and preserved in deep-water domains (Stow et al., 2001; Mollenhauer et al. 2007; Baudin et al., 2017). In this study we tried to understand the origin and the fate of the OM transported from the shallow to the deep-water domain of the Mozambique Channel.

RE6 data indicate that suspended sediments from the Zambezi slope are characterized by higher OI values (300 to 700 mg CO_2/g TOC), *i.e.* more oxidized samples, compared to suspended sediments from the deep-water Zambezi distal valley (150 to 300 mg CO_2/g TOC) (Fig. 3b). The Zambezi distal valley presents suspended sediments which are less oxidized compared to the Zambezi slope (Fig. 3b) and that show more affinity in terms of S2, TOC, HI and OI values with suspended sediments collected in the Tsiribihina submarine valley or even in the Majunga margin (Fig. 3b). According to these observations, the Zambezi distal valley would be preferentially fed by the Madagascar river system rather than from the Mozambique margin. This interpretation is consistent with the recent uplift caused by active tectonics across the Mozambique Channel (Deville et al., 2018) and that resulted in the partial closure of the main Zambezi turbidite channel near the western Bassas da India-Europa area (Fierens et al., 2019) (Fig. 1).

According to HI and OI values by Rock-Eval analysis, all the suspended sediments collected in the main physiographic provinces of the Mozambique Channel seem to be characterized by terrestrial OM. Based on average values of $\delta^{13}C$ between -21.5 and -22.1 ‰, a mixture of different sources (marine and terrestrial; Fig. 4) cannot be excluded. However, in the Betsiboka estuary (Fig. 1), values in this range were interpreted as a mixture of C3 and C4 derived OM, with negligible algal inputs (Ralison et al., 2008). Similar values were then found at the top of interface cores on the continental shelf (Pastor et al., 2020). The OM at seafloor and in core sediments shows characteristic Rock-Eval 6 values (*i.e.* HI and OI values) typical of terrestrial-derived OM (Fig. 6; 15). For comparison, the Monterey Canyon

17

in offshore central California shows an increase of marine OM influence in suspended sediments compared to core sediments (Mayer et al. 2019). The authors propose a scenario in which sediment density flows in the Monterey Canyon induce reworking and deposition of seafloor sediments, resulting in preferential consumption of marine OM in cores than in sediment trap compare to terrestrial OM. In the Mozambique Channel, the presence of turbidity currents in deep-water domains (Miramontes et al. 2019) can be regarded as responsible of low organic carbon burial efficiency (Mayer et al. 2019) which would explain a better preservation of marine OM in sediment traps and δ^{13}C values of mixed OM sources.

5.3 Preservation condition of the sedimentary OM

Sediment cores show that the OM is characterized by two HI groups: a first group with average HI values around 150 mg HC/g TOC (NW of Madagascar and in the Davie Ridge area), and a second HI group with average values around 75 mg HC/g TOC (Zambezi system) (Fig. 6). Considering that the suspended sediments collected in the Zambezi slope are already largely oxidized before deposition (Fig. 3b), we can assume that the different HI groups observed in the sediment cores (Fig. 6) are likely due to different oxidation conditions of an initial terrestrial OM, as an increase of OM oxidation can lead to higher OI and lower HI values (Baudin et al. 2017). Additional studies on palynofacies, carbon stable isotopes (δ^{13}C) of seafloor samples or organic petrography (e.g. optical analysis) could help to confirm this interpretation. We also compare REc results of suspended sediments, seafloor sediments and sediment cores to better assess preservation and transport conditions (Fig. 15). Suspended sediments contain the highest OM content (TOC values between 1.5 and 3.5%) both in the shallow water and in the deep-water domains (Fig. 3a; 15a). The OM seems to be transported over large distances and minimally affected by degradation processes. Along the Zambezi turbidite system, OM collected in sediment traps shows that it is preserved with higher TOC and HI and lower OI values (HI > 200 mg HC/g TOC, OI < 300 mg CO_2/g TOC) and transported by turbidite and/or bottom currents towards the deep-water domains (Fig. 15). However, below 2500 m of water depth, the OM content in seafloor sediments strongly decreases, especially in the distal depositional areas (Fig. 16). The decrease of TOC in seafloor sediments of the deep-water domain of the Mozambique Channel (Fig. 5) is particularly notable when compared with other turbidite systems such as the Orinoco river (Deville et al., 2015). The OM signature observed in the Orinoco abyssal plain (2000 to 4000 m of water depth) is similar to the Mozambique Channel (Fig. 3). However, the OM is better preserved in the recent sediments of the Orinoco abyssal plain which show TOC values

between 0.5% and 1.5%. We can also compare our findings with the Congo deep-sea fan where the OM is transported by turbidity currents to 5000 m of water-depth while preserving high values of TOC (~ 3.5 to 4%) (Baudin et al., 2017) (Fig. 3). Although the OM is well transported to the distal lobe of the Mozambique Channel as shown by suspended sediments (TOC between 1.5 and 2.6 %), it is strongly degraded at the water-sediment interface (Fig. 5). Therefore, we observe that the terrestrial OM sourced by the major rivers along the Mozambique and Madagascar margins reaches the deep-water domain of the Mozambique Channel but it is not preserved in the recent sediments. In contrast to the Orinoco or Congo turbidite systems, the Mozambique Channel does not seem to be an important sink for recent terrestrial OM. This is probably due to the activity of bottom water currents. Miramontes et al. (2019) have shown that the Mozambique Channel can be defined as a mixed turbidite-contourite system dominated by erosional processes at the seafloor induced by intense bottom currents. Therefore, the complexity of water circulation in the basin may be responsible for the remobilization of the OM which is then diluted and degraded (Fig. 5). This is also confirmed by the higher OPD in the distal depositional area of the Mozambique Channel (*e.g.* > 9 cm at MOZ1-MTB12) (Fig. 14) compared to the Congo turbidite system where measured OPD are < 1 cm (Pozzato et al. 2017).

5.2 Evolution of the OM deposition in the physiographic provinces of the Mozambique Channel

The mineralogical differences in samples from the Zambezi and Majunga slopes could indicate two different depositional environments which may affect preservation conditions (Table 2). The samples from the uppermost sediments of the Mozambique slope present mainly K-feldspar and mica but no aragonite and only small amounts of calcite (Fig. 9; Table 2). This is also characteristic of an oxidizing depositional environment which is consistent with the presence of iron oxides in both the mineral matrix and the calcified OM (Fig. 10). Pore-water profiles measured in the same sediment core show ferruginous conditions (excess in Fe^{2+}) and labile iron oxides are still present at depth at around 1% (Zindorf et al., 2021). This suggest that geochemical processes within the sedimentary column in this area are controlled by iron, even in the sulfate reduction and methane migration zones, and could explain the precipitation of iron oxide inside marine bioclasts. In contrast, the samples from the uppermost sediments of NW Madagascar are rich in aragonite, calcite and shell residues, with no or limited iron oxide (Fig. 11, Table 2). This is representative of reducing depositional environments in the uppermost cm of sediments. As presented in Pastor et al.

(2020), the Majunga slope is reached by flows of detrital iron oxides carried by the Betsiboka river. Therefore, the absence of iron oxides in the MOZ01-KSF12 sample, as revealed by EDS-SEM analysis, may be related to the consumption of iron oxides in reducing conditions to form pyrite in relation to upward methane-rich fluid migration (Pastor et al., 2020).

The comparison of analytical results obtained from suspended, seafloor and core samples suggests that OM is largely diluted and degraded in the first few centimeters of the water-sediment interface in areas of water depth higher than 2500 m (Fig. 15; 16). In these areas, oxygen was measured at least down to 8 cm in the sediments and OET reaches several thousand years (Table 3, Fig. 14). Indeed, in the deep-water area of the Mozambique Channel, important oxidation processes occurred in the uppermost sediments as confirmed by the decrease of the S2 peak (< 0.5 mg HC/g rock) and the TOC content (< 0.5%), coupled with an increase of OI (> 300 mg CO_2/g TOC) (Fig. 15). This is also confirmed by the thicker O_2-bearing zone in the uppermost sediments of the deep-water area of the Mozambique Basin along the distal Zambezi and Tsirihibina valleys (Fig. 14). These oxidizing conditions are interpreted by the conjugate effects of lower sedimentation rates (Table 3) and higher porosities of the sand-rich material of the Zambezi distal system (Fierens et al., 2019). This process is probably the result of the activity of important bottom currents (Miramontes et al., 2019) which are prone to maintain oxidizing conditions by the remobilization of the uppermost sediments and its OM (Fig. 15). Indeed, current velocities reach up to 50 cm.s^{-1} in the Zambezi valley at MPL2 (Fig. 1), 38 cm.s^{-1} in the Tsiribihina valley at MPL3 (Fig. 1) and 36 cm.s^{-1} in the Zambezi distal valley at MPL5 (Miramontes et al., 2019). Overall, these processes are responsible for higher oxygen exposure times ranging from a few years (7 to 172 yrs in the Mozambique and Madagascar margins) to thousands of years (up to 16,600 yrs in the Zambezi distal valley; Table 4).

Bottom currents have a major impact on the evolution of TOC (%) in the main physiographic provinces of the Mozambique Channel (Fig. 17). The OM is transported to the distal valley as indicated by higher TOC values in suspended sediments (Fig. 17). However, the OM content rapidly decreases in the first few centimeters of sediments due to deep and cold water currents (Miramontes et al. 2019) that induce erosion, reworking and deposition of sediments (Stow et al. 2018). This process is also confirmed by deeper OPD (Fig. 17). In contrast, OM transported and deposited along the Majunga and Zambezi valleys is better preserved both in sediment traps and in core samples (Fig. 3a; Fig. 15). The presence of anticyclonic rings along the western Mozambique margin (Miramontes et al. 2019) can affect deep-water circulation

with alternating periods of strong bottom currents that result in seafloor erosion, sediment resuspension and higher oxidation of its OM. This process is observed in suspended sediments collected along the Zambezi slope (Fig. 3 b) which contains terrestrial OM already largely oxidized before deposition. In contrast, the Majunga slope is characterized mainly by surface water circulation resulting in a less disturbed depositional environment, higher OM content at the seafloor and lower oxygen penetration depth (Fig. 17).

In the Mozambique Channel, important amount of mixed OM (TOC > 2%) is efficiently transported until the distal depositional areas (> 4000 m water depth). However, the OM is not well preserved in areas of water depth higher than 2500 m due to the presence of sediment flows and bottom currents (Miramontes et al. 2019) which induce higher OET and low OC burial efficiency. Therefore, the distal lobes of the Mozambique Channel are not regarded as a sink of terrestrial OC in the active carbon cycle.

6. Conclusion

In this work, we present the analysis of the organic matter evolution over a wide scale from shallow areas to deep-water domains of the Mozambique Channel. Analyses of OM collected from suspended sediments, seafloor sediments and cores (core length < 33 m of depth) allowed us to assess transport and degradation-preservation conditions. The Mozambique Channel accommodates large amounts of terrestrial OM issued from the Madagascar and Mozambique margins. The highest OM content in core sediments has been found in the Majunga area (TOC ~ 1.4%), offshore Madagascar, and on the Zambezi slope (TOC ~ 1.1%), offshore Mozambique. Suspended sediments from the deep-water domain of the Zambezi turbidite system show a relatively high content of OM (TOC ~ 2%) which is less oxidized compared to the Zambezi slope. Rock-Eval 6 results suggest that the deep-water domains of the Mozambique Channel are preferentially fed with terrestrial OM issued from the Madagascar river system rather than from Mozambique. We therefore can assume that in the deeper parts of the Mozambique Channel, the OM is efficiently transported by turbidity and/or contour currents and deposited in the turbidite system of the deep-water area of the Mozambique Basin while preserving higher amounts of poorly oxidized OM. However, the deposited OM in seafloor sediments is largely oxidized. This process is probably related to the conjugate effects of lower sedimentation rates and higher porosity of the sand-rich material present in the Zambezi distal system. Consequently, the Mozambique Channel does not seem to be an important sink of terrestrial organic matter in contrast to other turbidite systems. The activity of important marine currents is responsible for erosion, reworking and remobilization of sediments and OM within at the sea bottom, leading to higher oxygen exposure time in the uppermost centimeters of the sediments.

Appendix A. Supplementary material

Supplementary Fig. S1. The three different types of sampling devices

Supplementary Fig. S2. $^{210}Pb_{xs}$ profiles measured on cores MOZ4-MTB4 and MOZ4-MTB5

References

Ahuva, A.L., Amos, B., Sass, E., 1993. Late Cretaceous upwelling system along the Southern Tethys Margin Israel Interrelationship between productivity, bottom water environments, and organic matter preservation. Paleoceanography 8, 5, 671–690.

Aminot, A., Kérouel, R., 2004. Hydrologie des écosystèmes marins. Paramètres et analyses. 335 p.

Balslev-Clausen, D., Dahl, T.W., Saad, N., Rosing, M.T., 2013. Precise and accurate delta C-13 analysis of rock samples using Flash Combustion-Cavity Ring Down Laser Spectroscopy. J. Anal. At. Spectrom. 28 (4), 516–523. doi:10.1039/C2JA30240C.

Barber, A., Brandes, J., Leri, A., Lalonde, K., Balind, K., Wirick, S., Wang, J., Gélinas, Y., 2017. Preservation of organic matter in marine sediments by inner-sphere interactions with reactive iron. Scientific Reports 7, 366, doi:10.1038/s41598-017-00494-0.

Baudin, F., Disnar, J-R., Martinez, P., Dennielou, B., 2010. Distribution of the organic matter in the channel-levees systems of the Congo mud-rich deep-sea fan (West Africa). Implication for deep offshore petroleum source rocks and global carbon cycle. Marine and Petroleum Geology 27, 5, 995–1010. doi:10.1016/j.marpetgeo.2010.02.006.

Baudin, F., Stetten, E., Schnyder, J., Charlier, K., Martinez, P., Dennielou, B., Droz, L., 2017. Origin and distribution of the organic matter in the distal lobe of the Congo deep-sea fan – A Rock-Eval survey. Deep Sea Research Part II: Topical Studies in Oceanography 142, 75–90. doi:10.1016/j.dsr2.2017.01.008.

Behar, F., Beaumont, V., B. Penteado, H. L. de, 2001. Rock-Eval 6 Technology. Performances and Developments. Oil & Gas Science and Technology 56 2, 111–134. doi:10.2516/ogst:2001013.

Berner, R. A. (1982). Burial of organic carbon and pyrite sulfur in the modern ocean: its geochemical and environmental significance. *Am. J. Sci.;(United States)*, *282*. DOI: doi:10.2475/ajs.282.4.451

Berthois, L., Crosnier A., 1966. Etude dynamique de la sédimentation au large de l'estuaire de la Betsiboka. Cahiers O.R.S.T.O.M., sér. Océanogr. IV, 2.

Bouillon, S., Connolly, R.M., and Lee, S.Y. 2008. Organic matter exchange and cycling in mangrove ecosystems: recent insights from stable isotope studies. Journal of sea research, 59(1-2), 44-58. doi:10.1016/j.seares.2007.05.001.

Bourillet, J.F., Ferry, J.N., Bourges, P., 2013. PAMELA, Passive Margins Exploration Laboratories. doi:10.18142/236.

Bröder, L., Tesi, T., Andersson, A., Semiletov, I., and Gustafsson, Ö. 2018. Bounding cross-shelf transport time and degradation in Siberian-Arctic land-ocean carbon transfer. *Nature communications*, *9*(1), 1-8. doi:10.1038/s41467-018-03192-1

Burdige, D. J. 2005. Burial of terrestrial organic matter in marine sediments: A re-assessment. *Global Biogeochemical Cycles*, *19*(4). doi:10.1029/2004GB002368.

Burdige, D.J., 2007. Preservation of Organic Matter in Marine Sediments: Controls, Mechanisms, and an Imbalance in Sediment Organic Carbon Budgets? Chemical Reviews 107, 467-458. doi:10.1021/cr050347q.

Cowie, G. L., Hedges, J. I., & Calvert, S. E. 1992. Sources and relative reactivities of amino acids, neutral sugars, and lignin in an intermittently anoxic marine environment. *Geochimica et Cosmochimica Acta*, *56*(5), 1963-1978. doi:10.1016/0016-7037(92)90323-B.

Craig, H. (1953). The geochemistry of the stable carbon isotopes. Geochimica et cosmochimica acta, 3(2-3), 53-92. doi:10.1016/0016-7037(53)90001-5.

Deroo, G., Herbin, J. P., Roucaché, J., 1982. Organic geochemistry of upper Jurassic Cretaceous sediments from site-511, leg-71 Western South-Atlantic. Initial Reports of the Deep Sea Drilling Project, 71, 1001–1012.

Deville, E., Mascle, A., Callec, Y., Huyghe, P., Lallemant, S., Lerat, O., Mathieu, X., Padron de Carillo, C., Patriat, M., Pichot, T., Loubrieux, B., Granjeon, D. 2015. Tectonics and sedimentation interactions in the east Caribbean subduction zone. An overview from the Orinoco delta and the Barbados accretionary prism. Marine and Petroleum Geology 64, 76–103. doi:10.1016/j.marpetgeo.2014.12.015.

Deville, É., Guerlais, S-H., Callec, Y., Griboulard, R., Huyghe, P., Lallemant, S, Mascle, A., Noble, M.,Schmitz, J. and the CARAMBA research team, 2006. Liquefied vs Stratified Sedimentation Mobilization Processes: Insight from the South of the Barbados Accretionary Prism.Tectonophysics, 428, 33-47. doi:10.1016/j.tecto.2006.08.011.

Espitalie, J., Laporte, J.L., Madec, M., Marquis, F., Leplat, P., Paulet, J., 1977. Méthode rapide de caractérisation des roches mères, de leur potentiel pétrolier et de leur degré d'évolution. Rev. Inst. fr. petr., 32, 1, 23-42. doi:10.2516/ogst:1977002

Espitalié, J., Madec, M., Tissot, B., Mennig, J. J., Leplat, P., 1977. Source Rock Characterization Method for Petroleum Exploration. In. Offshore Technology Conference. OTC, 1977/1/1, Offshore Technology Conference, p. 6.

Espitalié, J., Senga Makadi, K., Trichet, J., 1984. Role of the mineral matrix during kerogen pyrolysis. Organic Geochemistry 6, 365–382. doi:10.1016/0146-6380(84)90059-7.

Espitalie, J., Deroo, G., Marquis, F., 1985. Rock-Eval pyrolysis and its applications. I Rev. Inst. fr. petr. 40, 5, 563–579.

Fierens, R., Droz, L., Toucanne, S., Raisson, F., Jouet, G., Babonneau, N., Miramontes, E., Landurain, S., Jorry, S., 2019. Late Quaternary geomorphology and sedimentary processes in the Zambezi turbidite system (Mozambique Channel). Geomorphology 334, 1–28. doi:10.1016/j.geomorph.2019.02.033.

Fontanier, C., Mamo, B., Toucanne, S., Bayon, G., Schmidt, S., Deflandre, B., Dennielou, B., Jouet, G., Garnier, E., Sakai, S., Lamas, R.M., Duros, P., Toyofuku, T., Salé, A., Belleney, D., Bichon, S., Boissier, A., Chéron, S., Pitel, M., Roubi, A., Rovere, M., Grémare, A., Dupré, S., Jorry, S.J., 2018. Are deep-sea ecosystems surrounding Madagascar threatened by land-use or climate change? Deep Sea Research Part I, Oceanographic Research Papers 131, 93-100. doi:10.1016/j.dsr.2017.11.011.

Gaillardet, J., Dupré, B., Louvat, P., & Allegre, C. J. 1999. Global silicate weathering and CO2 consumption rates deduced from the chemistry of large rivers. *Chemical geology*, *159*(1-4), 3-30. doi:10.1016/S0009-2541(99)00031-5.

Galy, V., Peucker-Ehrenbrink, B., Eglinton, T., 2015. Global carbon export from the terrestrial biosphere controlled by erosion. Nature 521, 204. doi:10.1038/nature14400.

Gordon, E. S., & Goñi, M. A. 2003. Sources and distribution of terrigenous organic matter delivered by the Atchafalaya River to sediments in the northern Gulf of Mexico. *Geochimica et Cosmochimica Acta*, *67*(13), 2359-2375. doi:10.1016/S0016-7037(02)01412-6.

Hare, A.A., Kuzyk, Z.Z.A., Macdonald, R.W., Sanei, H., Barber, D., 2014. Characterization of sedimentary organic matter in recent marine sediments from Hudson Bay, Canada, by Rock-Eval pyrolysis. Organic Geochemistry 68, 52–60. doi:10.1016/j.orggeochem.2014.01.007.

Hartnett, H. E., Keil, R.G., Hedges, J.I., Devol, A.H., 1998. Influence on oxygen exposure time on organic carbon preservation in continental margin sediments. Nature 391, 372-374. doi:10.1038/35351.

Hedges, J. I., Keil, R.G., 1995. Sedimentary organic matter preservation: an assessment and speculative synthesis. Marine Chemistry 49, 81-115. doi:10.1016/0304-4203(95)00008-F.

Hedges, J.I., Keil, R.G., Benner, R., 1997. What Happens to Terrestrial Organic Matter in the Ocean? Organic Geochemistry 27, 5/6, 195–212. doi:10.1016/S0146-6380(97)00066-1.

Hedges; I. J.; Clark, W.A., Come, G.L. 1988. Organic Matter Sources to the Water Column and surficial sediments of a marine bay. In *Limnol. Oceanogr.*, 1988, pp. 1116–1136. doi:10.4319/lo.1988.33.5.1116

Henrichs, S. M., Farrington, J. W., 1984. Peru upwelling region sediments near 15S. Remineralization and accumulation of organic matter. Limnology and Oceanography 29, 1–19. doi:10.4319/lo.1984.29.1.0001.

Jahnke, R. A. 1990. Early diagnosis and recycling of biogenic debris at the seafloor, Santa Monica Basin, California. J. Mar. Res. 48, 413–436. doi:10.1357/002224090784988773

Jouet, G., Deville, E., 2015. PAMELA-MOZ04 cruise, R/V Pourquoi Pas? doi:10.17600/15000700.

Keil, R. G., Hu, F. S., Tsamakis, E. C. & Hedges, J. I. 1994. Pollen in marine sediments as an indicator of oxidation of organic matter. *Nature* **369**, 639–641.

Keil, R. G., Dickens, A. F., Arnarson, T., Nunn, B. I. & Devol, A. H. (2004). What is the oxygen exposure time of laterally transported organic matter along the Washington margin?. Marine Chemistry, 92(1-4), 157-165. doi:10.1016/j.marchem.2004.06.024.

Khripounoff, A., 2017. PAMELA-MOZ08 cruise, R/V Antea. doi:10.17600/17003900.

Kohn, M. J. (2010). Carbon isotope compositions of terrestrial C3 plants as indicators of (paleo) ecology and (paleo) climate. *Proceedings of the National Academy of Sciences*, *107*(46), 19691-19695. doi:10.1073/pnas.1004933107.

Lafargue, E., Marquis, F., Pillot, D., 1998. Rock-Eval 6 Applications in Hydrocarbon Exploration, Production, and Soil Contamination Studies. Rev. Inst. Fr. Pét. 53, 4, 421–437. doi:10.2516/ogst:1998036.

Maier, K. L., Rosenberger, K. J., Paull, C. K., Gwiazda, R., Gales, J., Lorenson, T., ... & Cartigny, M. J. 2019. Sediment and organic carbon transport and deposition driven by internal tides along Monterey Canyon, offshore California. *Deep Sea Research Part I: Oceanographic Research Papers*, *153*, 103108. doi:10.1016/j.dsr.2019.103108.

Mignard, S. L. A., Mulder, T., Martinez, P., Charlier, K., Rossignol, L., & Garlan, T. (2017). Deep-sea terrigenous organic carbon transfer and accumulation: Impact of sea-level variations and sedimentation processes off the Ogooue River (Gabon). *Marine and Petroleum Geology*, *85*, 35-53. doi:10.1016/j.marpetgeo.2017.04.009

Miramontes, E., Penven, P., Fierens, R., Droz, L., Toucanne, S., Jorry, S.J., 2019. The influence of bottom currents on the Zambezi Valley morphology (Mozambique Channel, SW Indian Ocean). In situ current observations and hydrodynamic modelling. Marine Geology 410, 42–55. doi:10.1016/j.margeo.2019.01.002.

Mollenhauer, G., Inthorn, M., Vogt, T., Zabel, M., Sinninghe Damsté, J. S., & Eglinton, T. I. 2007. Aging of marine organic matter during cross-shelf lateral transport in the Benguela upwelling system revealed by compound-specific radiocarbon dating. *Geochemistry, Geophysics, Geosystems*, *8*(9). doi:10.1029/2007GC001603.

Mueller, C. O., Jokat, W., 2019. The initial Gondwana break-up: A synthesis based on new potential field data of the Africa-Antarctica Corridor. Tectonophysics, 750, 301–328. doi:10.1016/j.tecto.2018.11.008.

Müller, P. J., Suess, E. 1979. Productivity, sedimentation rate, and sedimentary organic matter in the oceans. I. Organic carbon preservation. Deep-Sea Res. A 26, 1347–1362. doi:10.1016/0198-0149(79)90003-7.

Nieto-Cid, M., Alvarez-Salgado, A., Pérez, F.F., 2006. Microbial and Photochemical reactivity of fluorescent dissolved organic matter in a coastal upwelling system. Limnology and Oceanography 51, 3, 1391–1400. doi:10.2307/3841185

Olu, K, 2014. PAMELA-MOZ01 cruise, R/V L'Atalante.

Pastor, L., Deflandre, B., Viollier, E., Cathalot, C., Metzger, E., Rabouille, C., Escoubeyrou, K., Lloret, E., Pruski, A.M., Vetion, G., Desmalades, M., Buscail, R., and Gremare, A. (2011). "Influence of the organic matter composition on benthic oxygen demand in the Rhone River prodelta (NW Mediterranean Sea)." Continental Shelf Research **31**(9): 1008-1019. doi:10.1016/j.csr.2011.03.007.

Pastor, L., Brandily, C., Schmidt, S., Miramontes, E., Péron, M., Apperé, D., Besson, S., Boissier, A., Jouet, G., 2020. Modern sedimentation and geochemical imprints in sediments from the NW Madagascar margin. Marine Geology, 426, 106184. doi:10.1016/j.margeo.2020.106184

Pedersen, T.F., Calvert, S.E., 1990. Anoxia vs. Productivity. What Controls the Formation of Organic-Carbon-Rich Sediments and Sedimentary Rocks?. AAPG Bulletin 74, 4, 454–466. doi:10.1306/0C9B282B-1710-11D7-8645000102C1865D.

Pelegrí, J.L., Arístegui, J., Cana, L., González-Dávila, M., Hernández-Guerra, A., Hernández-León, S., 2005. Coupling between the open ocean and the coastal upwelling region off northwest Africa. Water recirculation and offshore pumping of organic matter. Journal of Marine Systems 54, 1-4, 3–37. doi:10.1016/j.jmarsys.2004.07.003.

Pillot, D., Deville, E., Prinzhofer, A., 2014. Identification and Quantification of Carbonate Species Using Rock-Eval Pyrolysis. Oil & Gas Science and Technology 69, 2, 341–349. doi:10.2516/ogst/2012036.

Pozzato, L., Cathalot, C., Berrached, C., Toussaint, F., Stetten, E., Caprais, J.C., Pastor, L., Olu-Leroy, K., and Rabouille, C. 2017. Early diagenesis in the Congo deep-sea fan sediments dominated by massive terrigenous deposits: Part I–Oxygen consumption and organic carbon mineralization using a micro-electrode approach. Deep Sea Research Part II: Topical Studies in Oceanography, 142, 125-138. doi:10.1016/j.dsr2.2017.05.010.

Rabinowitz, P.D., Coffin, M.F., Falvey, D., 1983. The Separation of Madagascar and Africa. Science 220, 4592, 67–69. doi:10.1126/science.220.4592.67.

Rabouille, C., Caprais, J. C., Lansard, B., Crassous, P., Dedieu, K., Reyss, J. L., and Khripounoff, A. 2009. Organic matter budget in the Southeast Atlantic continental margin close to the Congo Canyon: In situ measurements of sediment oxygen consumption. *Deep Sea Research Part II: Topical Studies in Oceanography*, 56(23), 2223-2238.

Ralison, O.H., Borges, A.V., Dehairs, F., Middelburg, J.J., and Bouillon, S. (2008). Carbon biogeochemistry of the Betsiboka estuary (north-western Madagascar). *Organic Geochemistry*, *39*(12), 1649-1658. doi:10.1016/j.orggeochem.2008.01.010.

Regnier, P., Friedlingstein, P., Ciais, P. *et al.* 2013. Anthropogenic perturbation of the carbon fluxes from land to ocean. *Nature Geosci* 6, 597–607. doi:10.1038/ngeo1830.

Revsbech, N.P., 1989. An oxygen microsensor with a guard cathode. Limnology and Oceanography 34, 2, 474-478. doi:10.4319/lo.1989.34.2.0474

Romankevich, E.A., Vetrov, A.A., Peresypkin, V.I., 2009. Organic matter of the world ocean. Russ. Geol. Geophys. 50, 299e307. doi:10.1016/j.rgg.2009.03.013.

Schlesinger, W.H., Melack, J.M., 1981. Transport of organic carbon in the world's rivers. Tellus 33, 172e187. doi:10.1111/j.2153-3490.1981.tb01742.x.

Schmidt, S., De Deckker, P., 2015. Present-day sedimentation rates on the southern and southeastern Australian continental margins. Australian Journal of Earth Sciences 62, 143-150. doi:10.1080/08120099.2015.1014846.

Stow, D.A.V., Huc, A. Y., Bertrand, P., 2001. Depositional Processes of Black Shales in Deep Water. Marine and Petroleum Geology 18, 491–498. doi:10.1016/S0264-8172(01)00012-5.

Stow, D., Smillie, Z., & Esentia, I. P. (2018). Deep-Sea bottom currents: Their nature and distribution. In *Encyclopedia of ocean sciences: earth systems and environmental sciences*. doi:10.1016/B978-0-12-409548-9.10878-4.

Suess, E., 1980. Particulate organic carbon flux in the oceans—surface productivity and oxygen utilization. Nature 288, 5788, 260. doi:10.1038/288260a0.

Thompson, J.O., Moulin, M., Aslanian, D., de Clarens, P., Guillocheau, F., 2019. New starting point for the Indian Ocean : Second phase of breakup for Gondwana. Earth-Science Reviews, 191, 26–56. doi:10.1016/j.earscirev.2019.01.018.

Vangriesheim, A., Khripounoff, A., Crassous, P., 2009. Turbidity events observed in situ along the Congo submarine channel. Deep-Sea Research Part II-Topical Studies in Oceanography 56, 23, 2208-2222. doi:10.1016/j.dsr2.2009.04.004.

Van Krevelen, D. W., 1950. Graphical-statistical method for the study of structure and reaction processes of coal. Fuel 29, 269–284.

Wakeham, S.G., Lee, C., Hedges, J.I., Hernes, P.J., Peterson, M.J., 1997. Molecular indicators of diagenetic status in marine organic matter. Geochimica et Cosmochimica Acta 61, 24, 5363–5369. doi:10.1016/S0016-7037(97)00312-8.

Wang, X. C., Druffel, E.R.M., Griffin, S., Lee, C., Kashgarian, M., 1998. Radiocarbon Studies of Organic Compound Classes in Plankton and Sediment of the Northeastern Pacific Ocean. Geochimica et Cosmochimica Acta 62, 8, 1365–1378. doi:10.1016/S0016-7037(98)00074-X.

Wiles, E., Green, A., Watkeys, M., Botes, R., Jokat, W., 2019. Submarine canyons of NW Madagascar: A first geomorphological insight. Deep Sea Research Part II: Topical Studies in Oceanography 161, 5-15. doi:10.1016/j.dsr2.2018.06.003.

Yeh, H.W., and Wang, W.M. 2001. Factors affecting the isotopic composition of organic matter. (1) Carbon isotopic composition of terrestrial plant materials. *Proceedings of the National Science Council, Republic of China. Part B, Life sciences*, 25(3), 137-147.

Zindorf, M., Rooze, J., Meile, C., März, C., Jouet, G., Newton, R., Brandily, C., and Pastor, L. 2021. The evolution of early diagenetic processes at the Mozambique margin during the last glacial-interglacial transition. *Geochimica et Cosmochimica Acta*, *300*, 79-94. doi:10.1016/j.gca.2021.02.024

7. FIGURES
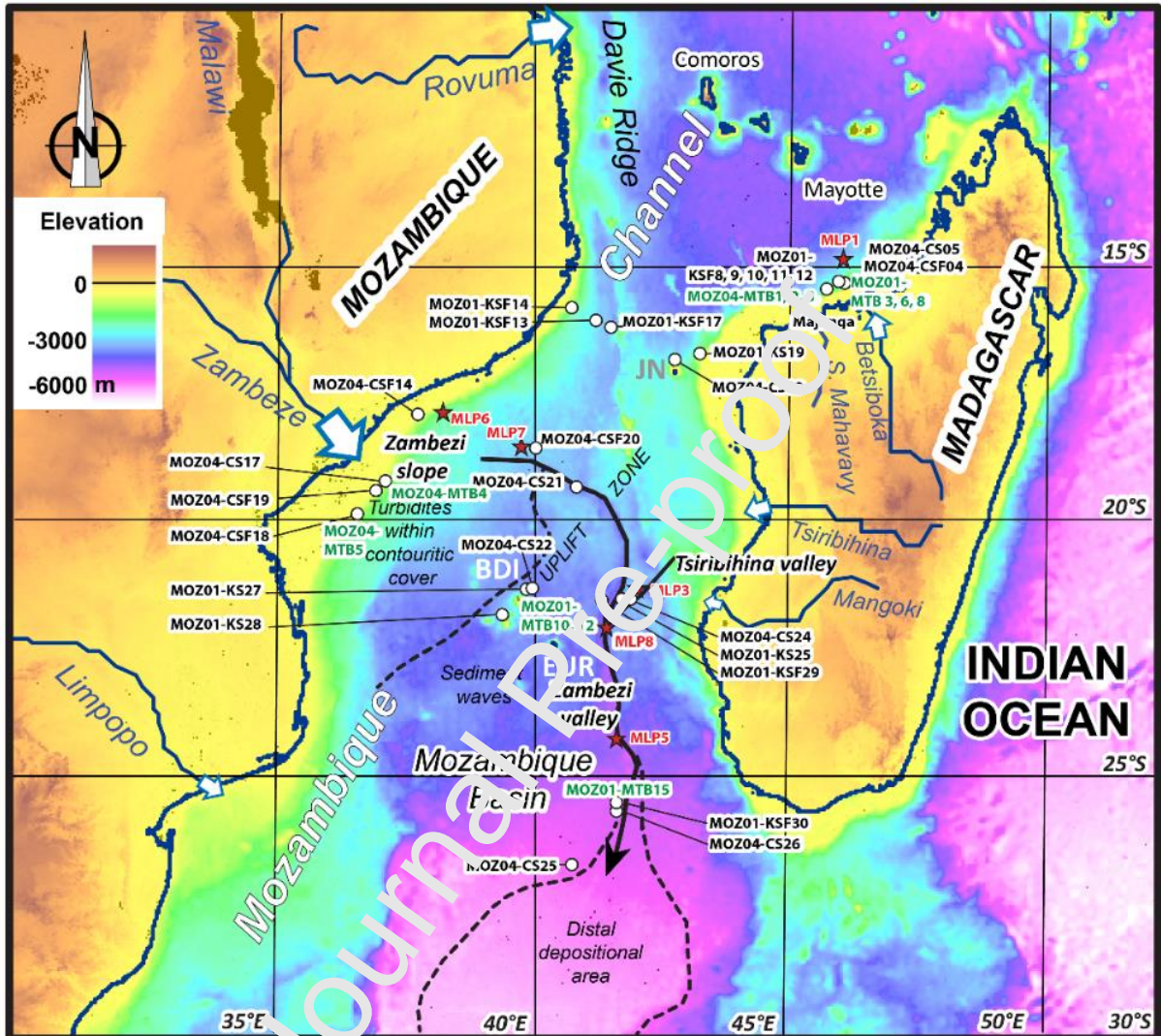
Fig. 1. Location map of the samples collected in the Mozambique Channel. The geological context is from Fierens et al. (2019). BDI: Bassas da India Island. EUR: Europa Island. JN: Juan de Nova. White dots and black letters indicate core sediments (CS, CSF, KSF and KS). White dots and green letters represent seafloor sediments (MTB). Red stars and red letters indicate the location of particle traps (MLP).
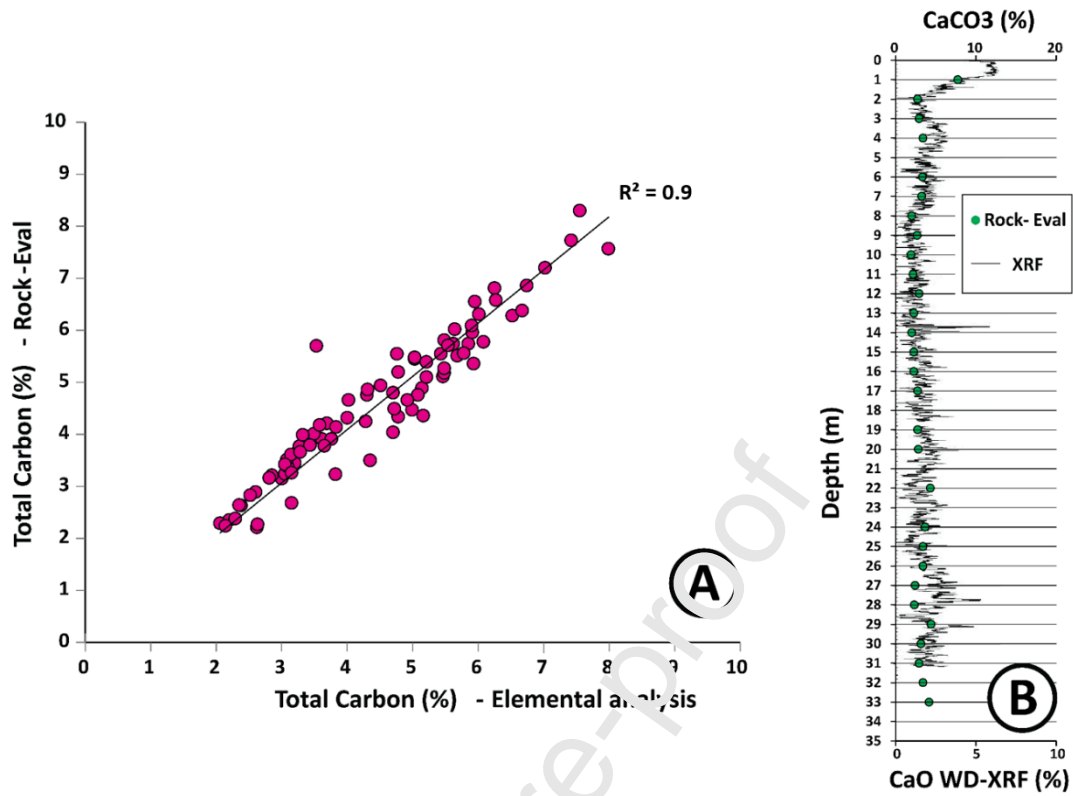
Fig. 2. (A) Cross-plot of Total Carbon determined from Rock-Eval and from LECO elemental analysis. (B) Comparison of calcite content (%) obtained by Rock-Eval method (Pillot et al., 2015) and Ca content from XRF analyses for a selected core sample (Pamela-MOZ04-CS17).

32
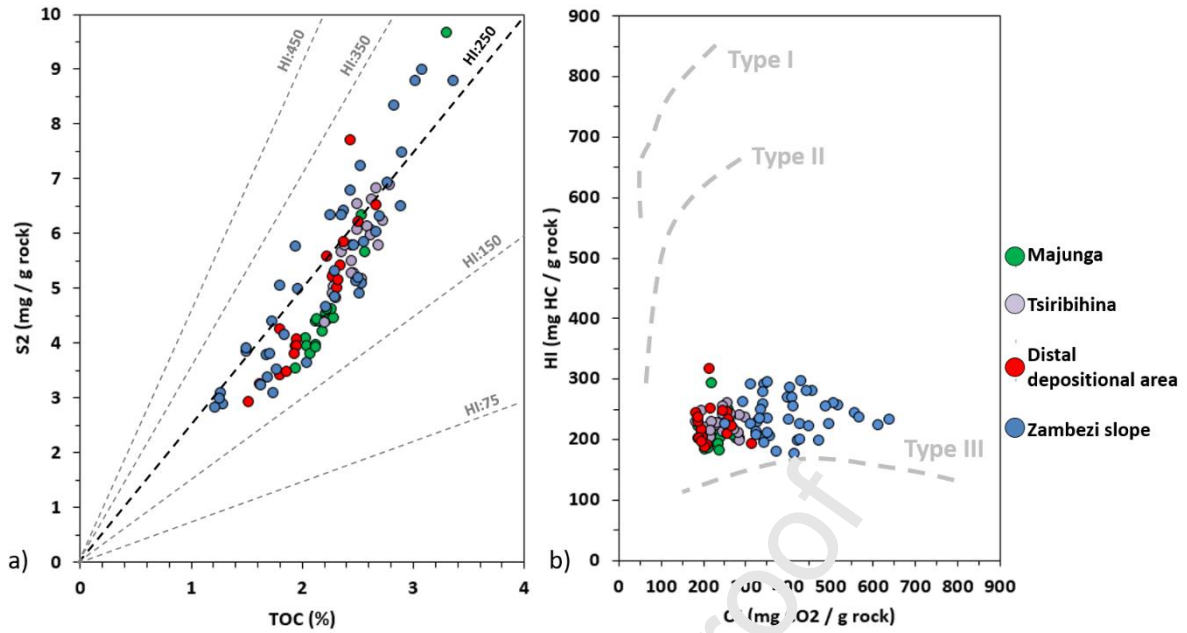
Fig. 3. Rock-Eval 6 results: (a) peak S2 *vs* Total Organic Carbon (TOC) content and (b) Hydrogen Index (HI) *vs* Oxygen Index (OI) values obtained from sedimentary organic matter of suspended sediments collected from the different physiographic provinces of the Mozambique Channel (Fig. 1).

33
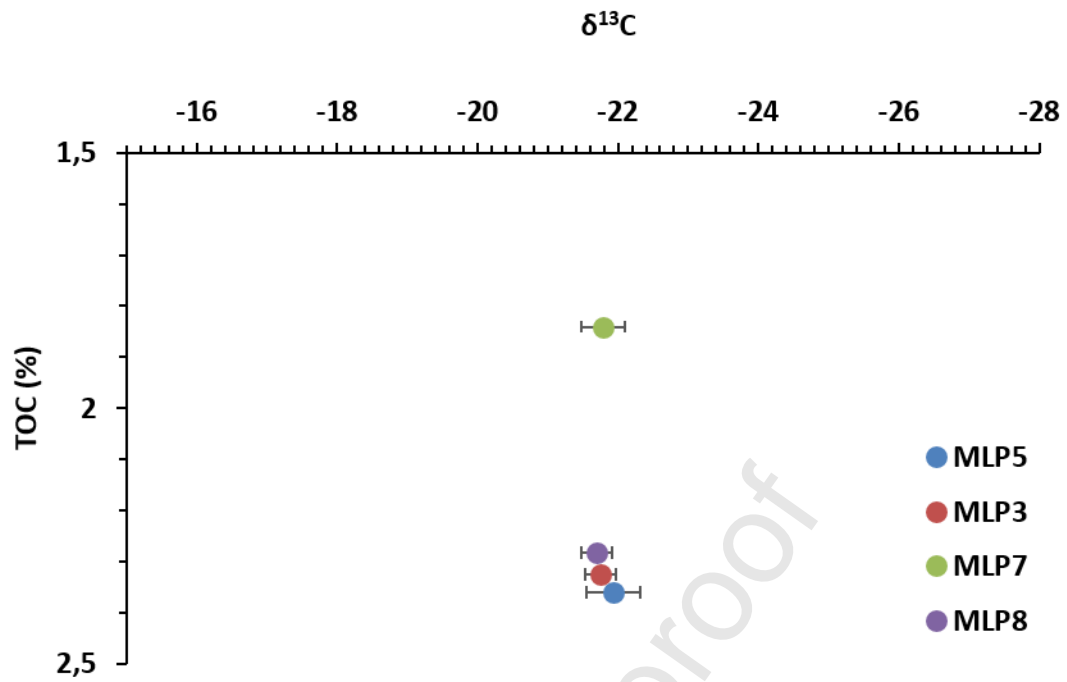
Fig. 4. Isotopic signature (δ^{13}C) of the organic carbon collected in particle traps (Fig. 1). Values are given as average for each sediment trap (Table 2). Horizontal lines represent the standard deviation.
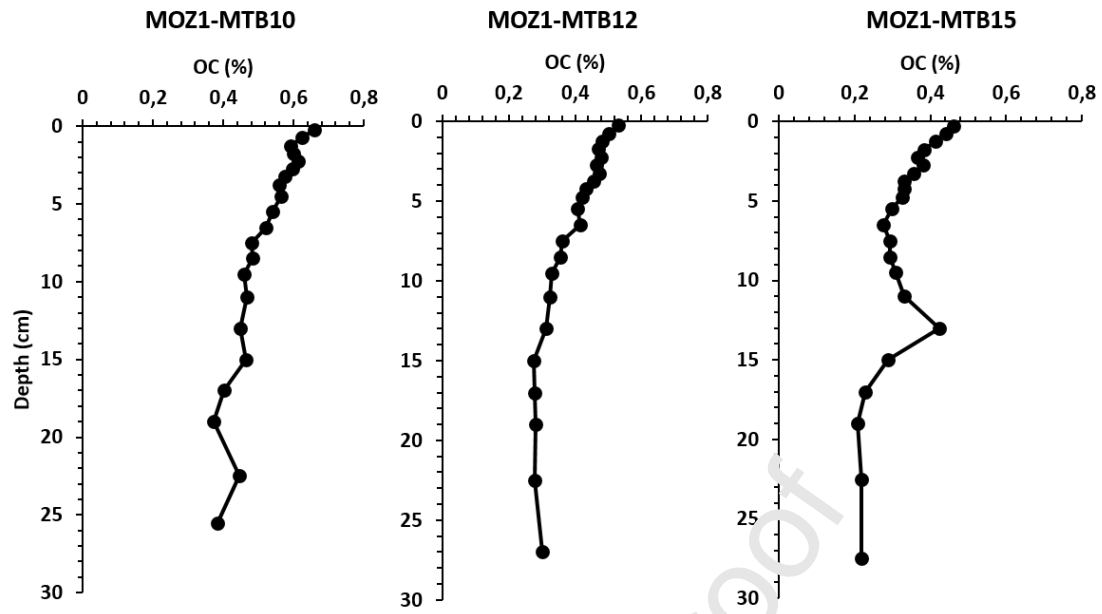
**Fig. 5**. Evolution of OC (%) *vs* depth from Leco analyzer for seafloor sediments (MTB) collected in the distal depositional areas.
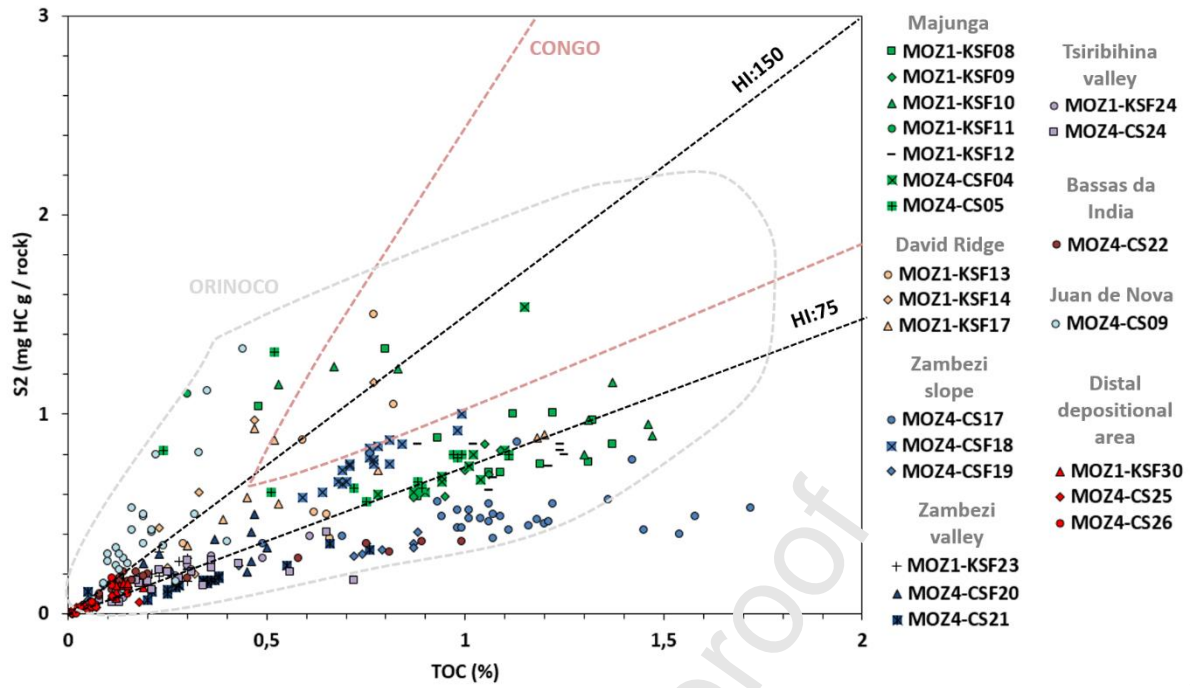
Fig 6. Rock-Eval 6 results (S2 vs TOC) of sedimentary organic matter from cores collected in the Mozambique channel, in comparison with Orinoco data range (from Deville et al., 2015) and Congo data range (from Baudin et al., 2017). Core locations are given in Figure 1.

36
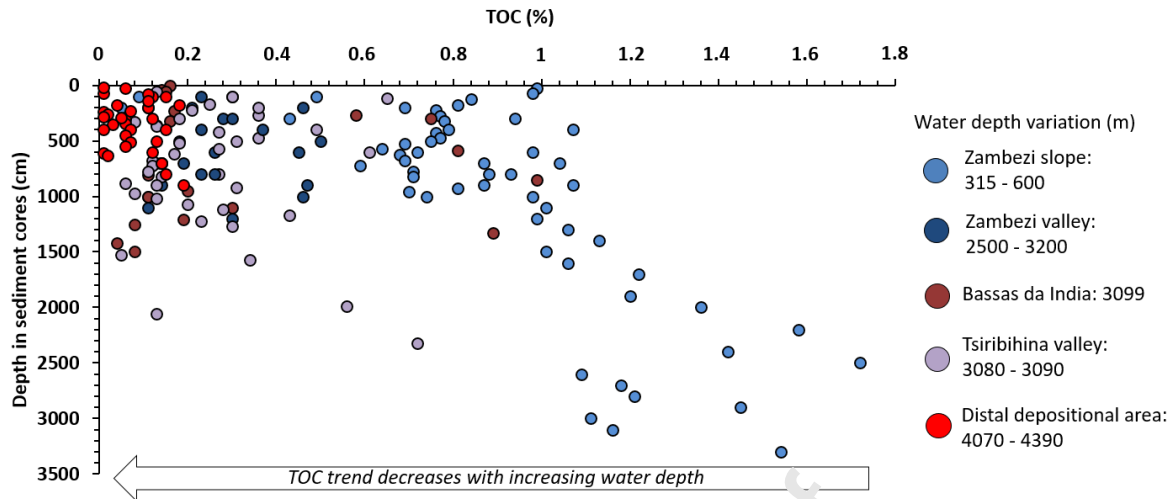
Fig 7. TOC (%) from RE6 analyses *vs* depth (m) in sediment cores sampled in the Zambezi turbidite system (Zambezi slope: MOZ4-CS17, MOZ4-CSF18, MOZ4-CSF19; Zambezi valley: MOZ1-KSF23, MOZ4-CSF20; Bassas da India: MOZ4-CS22; Tsiribihina valley: MOZ1-KSF24, MOZ4-CS24; Distal depositional area: MOZ1-KSF30, MOZ4-CS25, MOZ4-CS26) (for location map see Fig. 1). Note the strong TOC decrease towards the terminal distal channel.
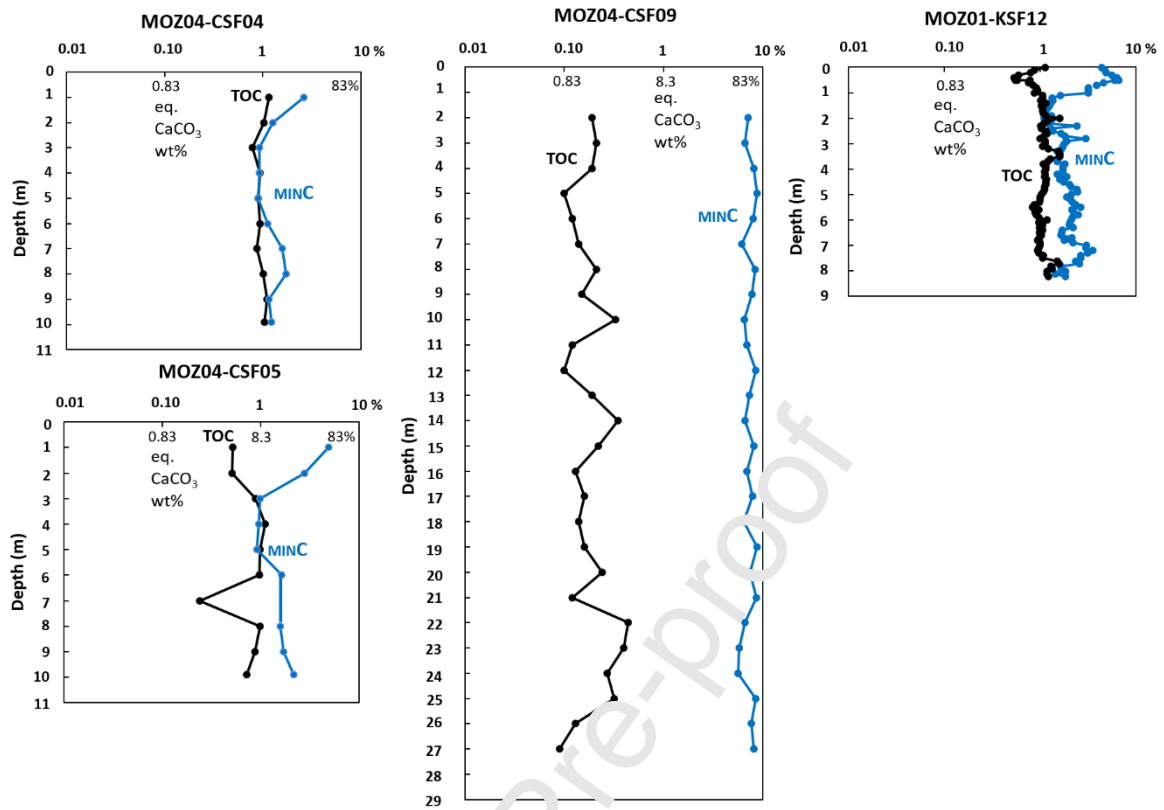
Fig. 8. Total Organic Carbon (TOC) and Inorganic Carbon (MINC) profiles *vs* depth from core samples in the Majunga margin (for sample locations see Fig. 1).
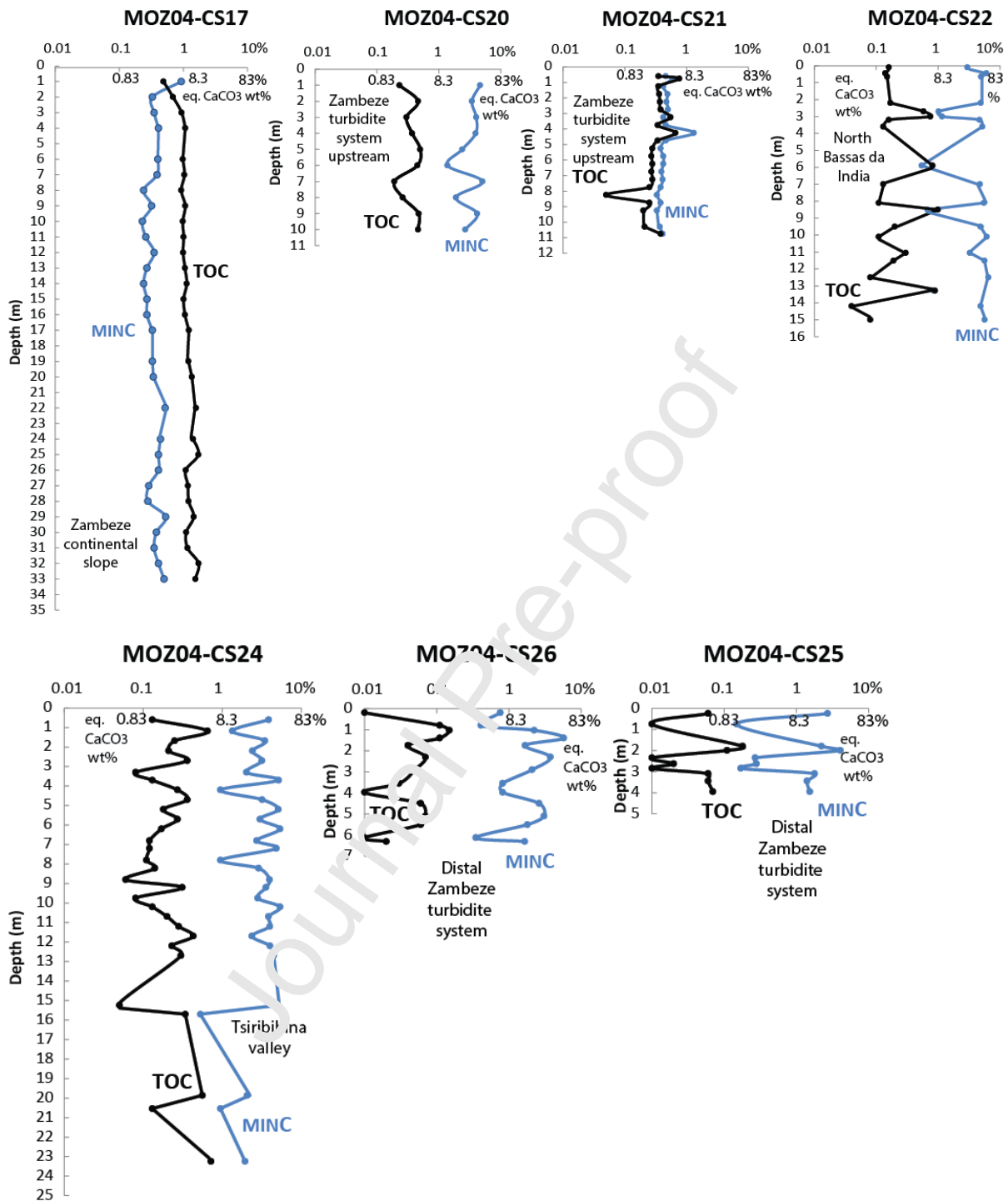
Fig. 9. Total Organic Carbon (TOC) and Inorganic Carbon (MINC) profiles *vs* depth along the Zambezi turbidite system (Mozambique continental slope and deep basin) (for sample locations see Fig. 1).
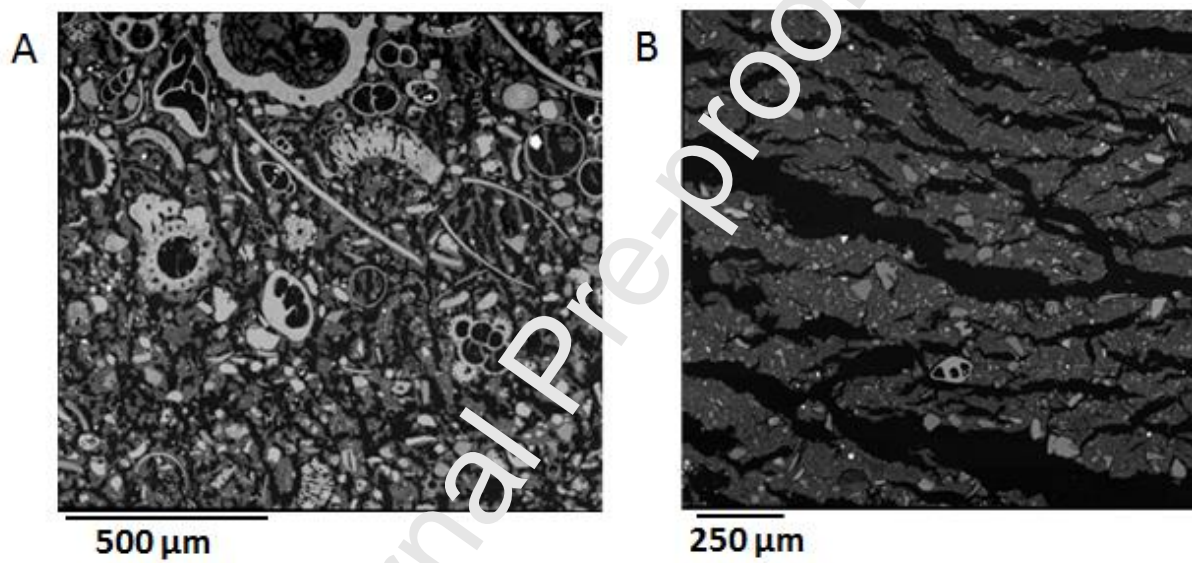
Fig. 10. SEM images illustrating the textural differences in the modern sediments from the Majunga slope, NW Madagascar (**A**) and from the Zambezi slope (**B**) (location is given in Fig. 1).
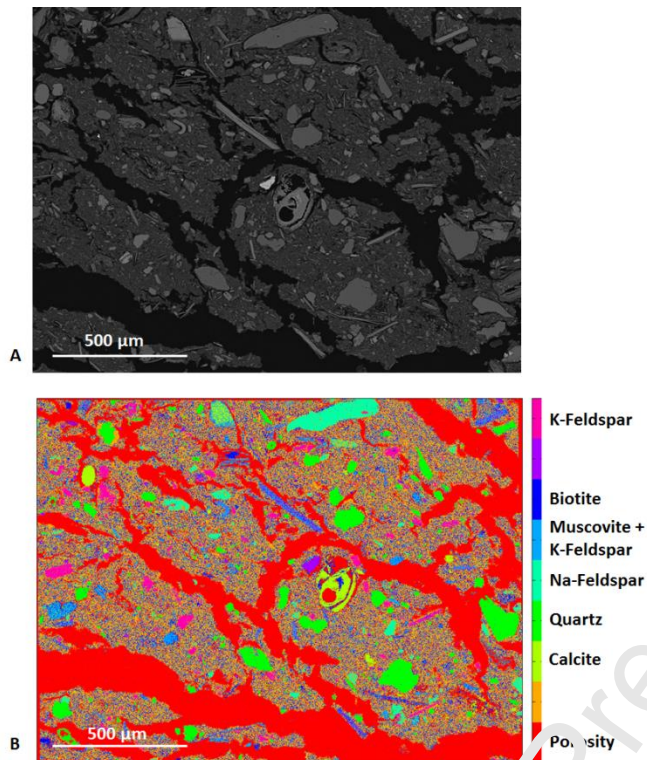
Fig. 11. EDS-SEM mineralogical mapping obtained by a statistical calculation (k-means clustering) on a sample of core Pamela MOZ04-CS17 (depth 78 cm bsf), Zambezi slope (for sample location see Fig. 1).
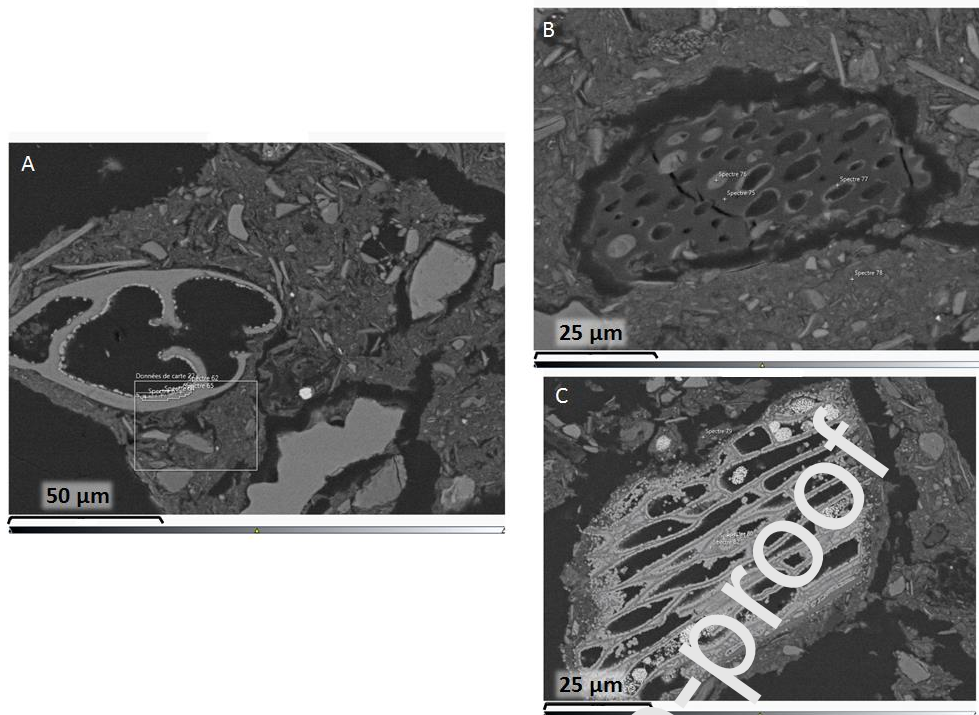
Fig. 12. SEM images illustrating (**A**) the presence of neo-formed iron oxides inside foraminifera test, (**B**) the presence of silica in OM, and (**C**) calcified OM. Samples from core Pamela-MOZ04-CS17, Zambezi valley (for sample location see Fig.1).
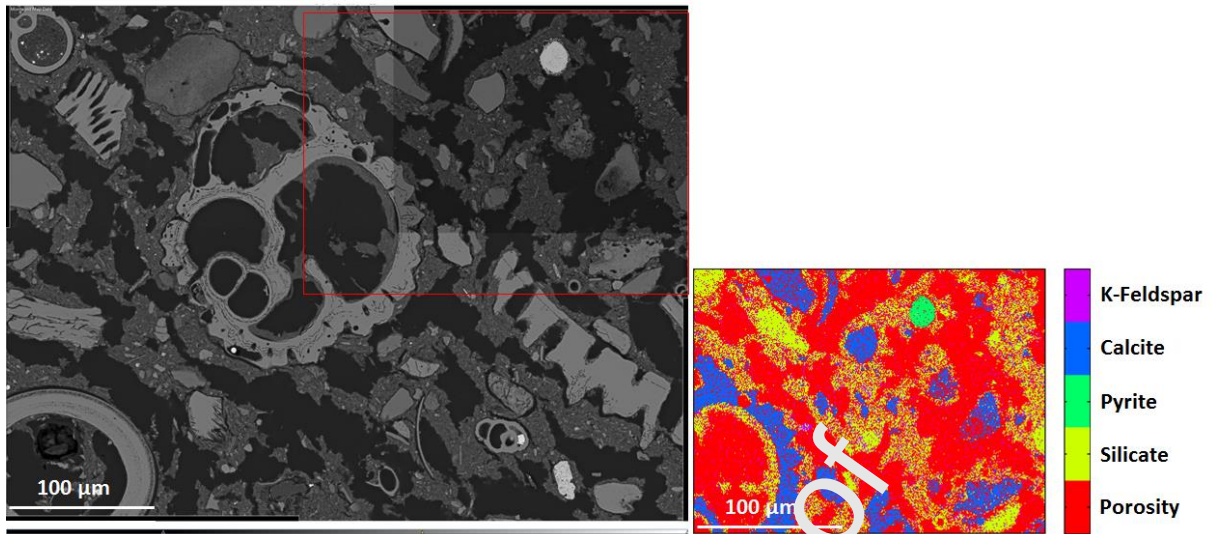
Fig. 13. Mineralogical mapping of a sample of core Pamela-MOZ01-KSF12 (depth 54 cm bsf), Majunga slope, NW Madagascar (for sample location see Fig. 1).
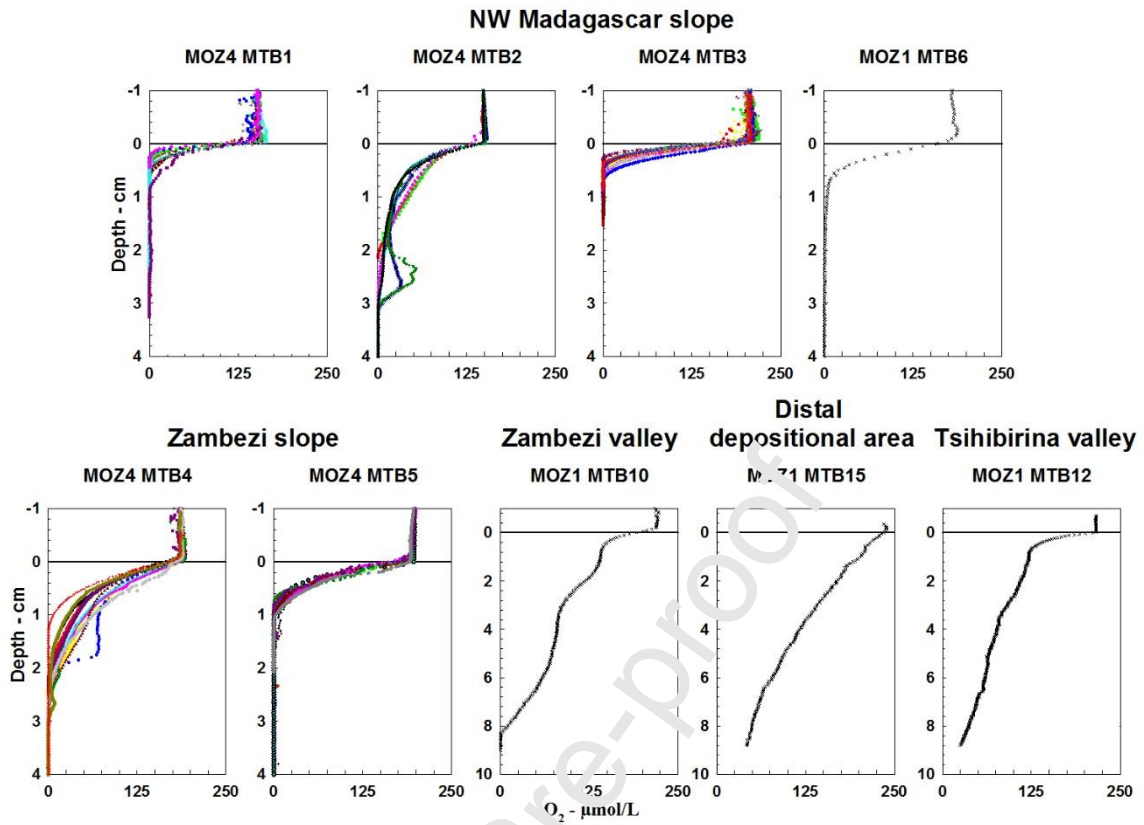
Fig. 14. Oxygen profiles measured on interface cores collected in the Mozambique Channel (for sample locations see Fig. 1).
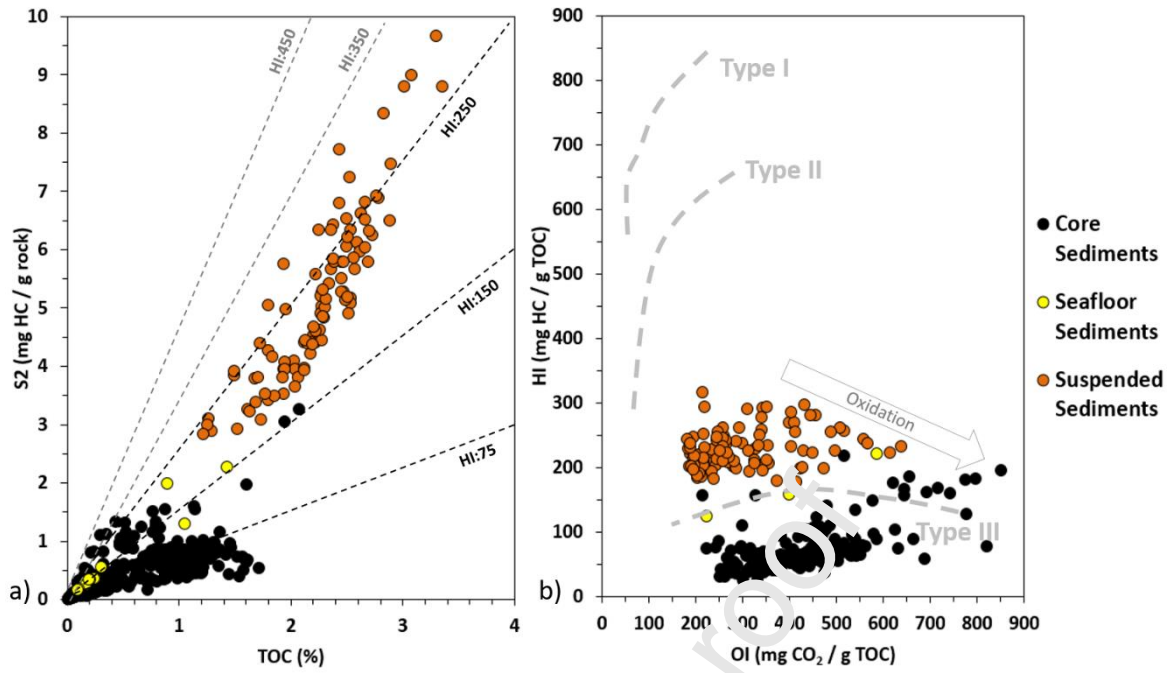
Fig. 15. Rock-Eval 6 results obtained on sedimentary organic matter from core sediments, seafloor sediments and suspended sediments collected in the Mozambique Channel. a) S2 *vs* TOC; b) HI *vs* OI.
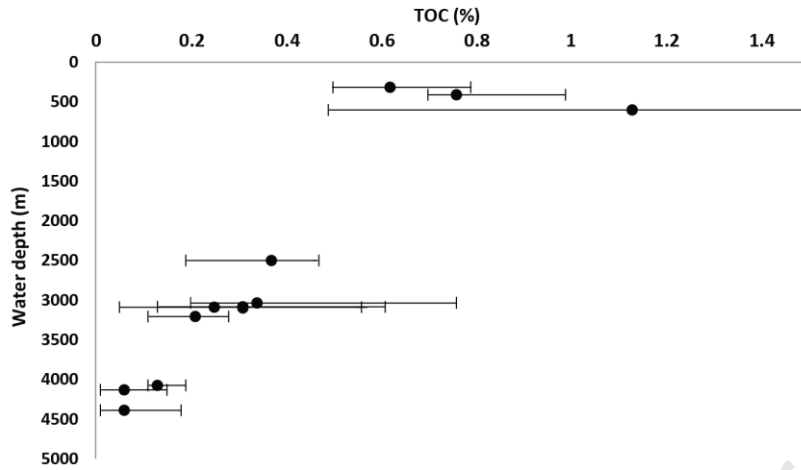
Fig. 16. TOC (%) as a function of water depth (m) along the Zambezi turbidite system. TOC is presented as average value in each core, with minimum and maximum values (Table 1).
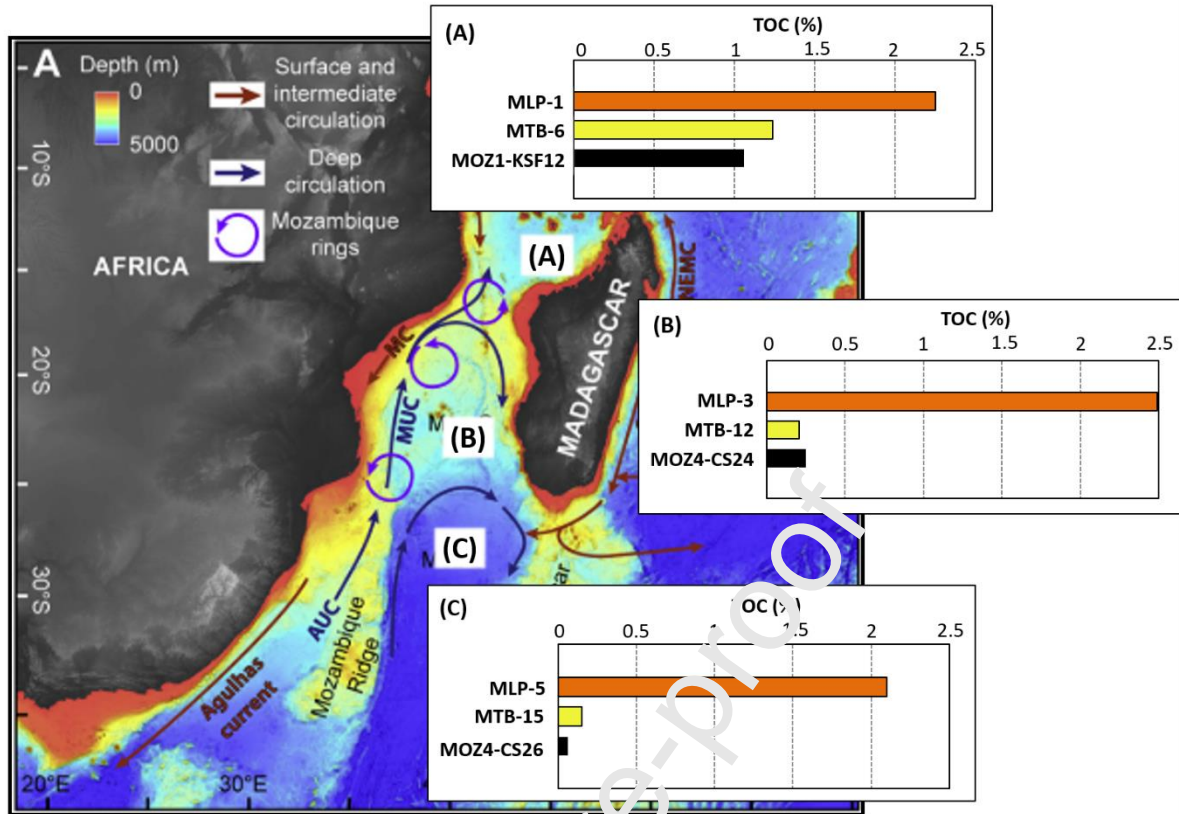
Fig. 17. Average TOC (%) for representative suspended sediments (orange bar), seafloor sediments (yellow bar) and core sediments (black bar) in the main physiographic provinces of the Mozambique Channel: (A) Mahanga slope (735 – 789 m water depth); (B) Tsiribihina valley (3089 – 3415 m water depth); (C) Distal depositional area (4054 – 4130 m water depth). The bathymetric map of the South East Indian Ocean shows the main circulation patterns observed the Mozambique Channel (modified after Miramontes et al. 2019) (for sample locations see Fig. 1).

	Latitude °S	Longitude °E	Water depth m	Mean S2 mg HC/g rock	Mean S3 mg CO₂/g rock	Mean TOC %Wt	TOCmin %Wt	TOCmax %Wt	Mean Tmax °C	Mean HI mg HC/ g TOC	Mean OI mg CO₂/g TOC	nb. Meas.
MOZ1-KSF8	15,36752	45,98712	528	0.88	4.72	1.06	0.8	1.37	410	79.9	441.2	12
MOZ1-KSF9	15,36143	45,95630	760	0.69	4.6	0.98	0.87	1.09	391	70.8	472.8	10
MOZ1-KSF10	15,51918	45,71581	773	1	3.99	1.29	0.83	1.47	409	80.9	348	10
MOZ1-KSF11	15,51590	45,71387	806	2.46	3.56	1.44	0.3	2.08	404	156	272	3
MOZ1-KSF12	15,36352	45,96047	735	0.75	4.73	1.06	0.87	1.62	399	71.6	464	96
MOZ1-KSF13	16,18514	41,40799	2618	1.02	5.58	0.79	0.29	1.94	402	120.3	771.7	8
MOZ1-KSF14	15,83619	40,74369	1552	0.53	3.94	0.36	0.15	0.77	395	151	709	7
MOZ1-KSF17	16,20568	41,44814	2730	0.69	3.39	0.66	0.3	1.2	417	102.2	437	9
MOZ1-KSF23	21,53033	41,34588	206	0.2	3.43	0.21	0.11	0.28	357			12
MOZ1-KSF24	21,51834	41,86120	3084	0.22	2.78	0.31	0.13	0.61	381	64	554	9
MOZ1-KSF30	25,42679	41,59536	4076	0.12	2.28	0.13	0.11	0.19	364			9
MOZ4-CSF04	15,37050	45,95183	757	0.7	4.87	0.98	0.58	0.87	392	78	501	11
MOZ4-CS05	15,36513	45,93953	898	0.7	4.83	0.78	0.24	1.11	378	122	752	11
MOZ4-CS09	16,84670	42,75748	1909	0.43	5.17	0.2	0.1	0.44	398			26
MOZ4-CS17	19,21335	37,04798	602	0.5	2.63	1.13	0.49	1.72	344	45	314	28
MOZ4-CSF18	19,84385	36,51310	410	0.76	2.43	0.76	0.7	0.99	379	100	451	18
MOZ4-CSF19	19,38998	36,87213	315	0.28	2.48	0.2	0.5	0.79	369	42	375	10
MOZ4-CSF20	18,44643	39,93160	2501	0.31	4.36	0.37	0.19	0.47	367			10
MOZ4-CS21	19,33855	40,77837	3036	0.17	1.49	0.4	0.2	0.76	366	46	424	21
MOZ4-CS22	21,27402	39,93130	3099	0.2	2.87	0.31	0.04	0.99	344	42	364	20
MOZ4-CS24	21,51845	41,86132	3089	0.16	2.6	0.25	0.05	0.56	364	42	361	30
MOZ4-CS25	26,62197	40,71247	4388	0.03	1.39	0.06	0.01	0.18	259			10
MOZ4-CS26	25,56643	41,61643	4130	0.05	1.42	0.06	0.01	0.15	339			14
MLP 1	15,51933	45,71572	781	4.72	5.22	2.25	1.94	3.?	400	207	232	20
MLP 3	21,52106	41,83437	3415	5.73	6.03	2.49	2.2	2.?3	4?4	229	243	22
MLP 5	23,97512	41,47293	4054	4.31	4.63	2.1	1.52	2.67	409	224	245	18
MPL7	18,6898	39,71093	2833	5.74	8.83	2.43	1.63	3.36	414	233	373	23
MPL8	22,22217	41,2715	3450	4.69	8.01	1.88	1.22	2.83	415	248	451	18
MOZ1_MTB6	15,51913	45,71551	789	1.78	4.03	1.24	1.05	1.43	386	141	311	2
MOZ1_MTB8	15,36358	45,96081	740	1.99	5.27	0.9			409			1
MOZ1_MTB10	21,53058	41,34562	3205	0.455	3.56	0.28	0.25	0.31	371			2
MOZ1_MTB12	21,51842	41,8613	3082	0.31	3.03	0.21	0.17	0.24	369			2
MOZ1_MTB15	25,42687	41,59557	4074	0.25	1.22	0.15	0.1	0.2	345			4

Table 1. Rock Eval results for the core samples collected in the Mozambique channel.

MLP	OC (%)	$\delta^{13}C$ (‰)	nb Meas.
3	2.32	-21.75 ± 0.21	2
5	2.36	-21.93 ± 0.37	3
7	1.84	-21.79 ± 0.31	23
8	2.28	-21.69 ± 0.21	22

Table 2. Average OC (%) measured with Leco analyzer and isotopic signature of the sedimentary organic carbon for specific suspended sediments. MLP = trap location number, OC = organic carbon, $\delta^{13}C$ = isotopic signature with standard deviation, nb = number of measurements.

	Quartz	Calcite	Halite	Feldspars	Kaolinite	Dolomite	Mica	Aragonite	Pyrite
KSF12-S1-54	9.2	28.4	2.1	3.5	22.6	tr	8.7	24.1	tr
CS17-S1-78	19.9	2.1	1.1	16.7	39.2	tr	20.1	-	tr

Table 3. Qualitative study of the mineralogical composition of samples MOZ01-KSF12-S1-54 Madagascar NW slope and MOZ04-CS17-S1-78 Zambezi slope (in normalized %).

Area	Interface core	Lat (°S)	Long (°E)	Water depth (m)	OPD (mm)	SAR (cm yr-1)	OET (yr)
NW Madagascar margin	MOZ4-MTB3	15°21.695	45°57.3886	757	34^c	0.52^b	65
	MOZ1-MTB?	15°21.815	45°57.6485	740	10^c	0.45^c	22
	MOZ1-MTB6	15°31.?48	45°42.9309	789	17.5^a	2.49^a	7
	MOZ4-MTB1	15°?.??2	45°57.628	735	5 ± 2^c	0.45^c	11
	MOZ4-MTB2	15°21.6?3	45°57.378	754	28 ± 4^c	0.39^b	72
	MOZ4-MTB3	15°22.230	45°57.110	762	5 ± 1^c	0.59^b	8
Mozambique margin	MOZ4-MTB4	19°50.650	36°?.76?	412	24 ± 4^c	1.43^c	17
	MOZ4-MTB5	19°23.330	36°52.?90	316	11 ± 2^c	0.064^c	172
Zambezi channel	MOZ1-MTB10	21°31.835	41°26.73?4	?205	83^a	0.005^c	16600
Tsiribihina channel	MOZ1-MTB12	21°31.105	41°51.6780	3?82	110^a	0.012^c	9167
Zambezi distal channel	MOZ1-MTB15	25°25.612	41°35.7334	40?4	120^c		

Table 4. OPD: Oxygen penetration depths measured on interface cores; SAR: sediment accumulation rates based mainly on $^{210}Pb_{xs}$ profiles in interface cores (NW Madagascar slope and Mozambique slope), on ^{14}C dating (Zambezi valley) and from an estimation based on mass accumulation rates in a moored sediment trap (Tsihiribihina valley; see explanation in the text); OET: oxygen exposure times calculated in interface cores;

a. From Fontanier et al., 2016; b. From Pastor et al., 2020; c. This study ($^{210}Pb_{xs}$ profiles are plotted in the supplementary Fig. S2, Appendix A).

Declaration of interests

☒ The authors declare that they have no known competing financial interests or personal relationships that could have appeared to influence the work reported in this paper.

☐The authors declare the following financial interests/personal relationships which may be considered as potential competing interests:

...ater Depth m	Mean S2 mg HC/g rock	Mean S3 mg CO₂/g rock	Mean TOC %Wt	TOCmin %Wt	TOCmax %Wt	Mean Tmax °C	Mean HI mg HC/g TOC	Mean OI mg CO₂/g TOC	nb. Meas.
28	0.88	4.72	1.06	0.8	1.37	410	79.9	441.2	12
60	0.69	4.6	0.98	0.87	1.09	391	70.8	472.8	10
73	1	3.99	1.29	0.83	1.47	409	80.9	348	10
06	2.46	3.56	1.44	0.3	2.08	404	156	272	3
85	0.75	4.73	1.06	0.87	1.62	399	71.6	464	96
18	1.02	5.58	0.79	0.29	1.94	402	120.3	771.7	8
52	0.53	3.94	0.36	0.15	0.77	395	151	709	7
30	0.69	3.39	0.66	0.3	1.2	417	102.2	437	9
06	0.2	3.43	0.21	0.11	0.28	357			12
84	0.22	2.78	0.31	0.13	0.61	381	64	554	9
76	0.12	2.28	0.13	0.11	0.19	364			9
57	0.77	4.87	0.98	0.58	0.87	392	78	501	11
98	0.76	4.83	0.78	0.24	1.11	378	122	752	11
09	0.43	3.17	0.2	0.1	0.44	398			26
02	0.5	3.46	1.13	0.49	1.72	344	45	314	28
10	0.76	3.43	0.76	0.7	0.99	379	100	451	18
15	0.28	2.48	0.62	0.5	0.79	369	42	375	10
01	0.31	4.36	0.37	0.19	0.47	367			10
36	0.17	1.49	0.34	0.2	0.76	366	46	424	21
99	0.2	2.87	0.31	0.04	0.9	344	42	364	20
89	0.16	2.6	0.25	0.05	0.6	364	42	361	30
88	0.03	1.39	0.06	0.01	0.18	259			10
30	0.05	1.42	0.06	0.01	0.15	339			14
81	4.72	5.22	2.25	1.94	3.3	400	207	232	20
15	5.73	6.03	2.49	2.2	2.73	414	229	243	22
54	4.31	4.63	2.1	1.52	2.67	409	224	245	18
33	5.74	8.83	2.43	1.63	3.36	414	233	373	23
50	4.69	8.01	1.88	1.22	2.83	415	248	451	18
89	1.78	4.03	1.24	1.05	1.43	386	141	311	2
40	1.99	5.27	0.9			409			1
05	0.455	3.56	0.28	0.25	0.31	371			2
82	0.31	3.03	0.21	0.17	0.24	369			2
74	0.25	1.22	0.15	0.1	0.2	345			4

Table 1. Rock Eval results for the core samples collected in the Mozambique channel.

54

Table 2. Average OC (%) measured with Leco analyzer and isotopic signature of the sedimentary organic carbon for specific suspended sediments. MLP = trap location number, OC = organic carbon, $\delta^{13}C$ = isotopic signature with standard deviation, nb = number of measurements.

MLP	OC	$\delta^{13}C$	nb Meas.
	(%)	(‰)	
3	2.32	-21.75 ± 0.21	2
5	2.36	-21.93 ± 0.37	3
7	1.84	-21.79 ± 0.31	23
8	2.28	-21.69 ± 0.21	22

Table 3. Qualitative study of the mineralogical composition of samples MOZ01-KSF12-S1-54 Madagascar NW slope and MOZ04-CS17-S1-78 Zambezi slope (in normalized %).

	Quartz	Calcite	Halite	Feldspars	Kaolinite	Dolomite	Mica
KSF12-S1-54	9.2	28.4	2.1	3.5	22.6	tr	8.7
CS17-S1-78	19.9	2.1	1.1	16.7	39.2	tr	20.1

Table 4. OPD: Oxygen penetration depths measured on interface cores; SAR: sediment accumulation rates based mainly on $^{210}Pb_{xs}$ profiles in interface cores (NW Madagascar slope and Mozambique slope), on ^{14}C dating (Zambezi valley) and from an estimation based on mass accumulation rates in a moored sediment trap (Tsihiribihina valley; see explanation in the text); OET: oxygen exposure times calculated in interface cores;

a. From Fontanier et al., 2016; b. From Pastor et al., 2020; c. This study ($^{210}Pb_{xs}$ profiles are

Area	Interface core	Lat (°S)	Long (°E)	Water depth (m)	OPD (mm)
NW Madagascar margin	MOZ1-MTB3	15°21.695	45°57.3886	757	34[c]
	MOZ1-MTB8	15°21.815	45°57.6485	740	10[c]
	MOZ1-MTB6	15°31.148	45°42.9309	789	17.5[a]
	MOZ4-MTB1	15°21.812	45°57.628	735	5 ± 2[c]
	MOZ4-MTB2	15°21.685	45°57.378	754	28 ± 4[c]
	MOZ4-MTB3	15°22.230	45°57.110	762	5 ± 1[c]
Mozambique margin	MOZ4-MTB4	19°50.650	36°30.765	412	24 ± 4[c]
	MOZ4-MTB5	19°53.330	36°52.390	316	11 ± 2[c]
Zambezi channel	MOZ1-MTB10	21°31.835	41°20.7374	3205	83[a]
Tsiribihina channel	MOZ1-MTB12	21°31.105	41°51.6780	3082	110[a]
Zambezi distal channel	MOZ1-MTB13	25°25.612	41°35.7334	4074	120[c]

plotted in the supplementary Fig. S2, Appendix A).

HIGHLIGHTS

- Origin and deposition of the Organic Matter in the main physiographic provinces of the Mozambique Channel
- Rock-Eval 6 data and δ^{13}C isotopic signature to determine the variability of OM composition within suspended, seafloor and core sediments
- EDS-SEM analysis, Sediment Accumulation Rates and Oxygen Exposure Times to assess the preservation condition of the OM in the Mozambique Channel
- Important bottom currents are prone to maintain higher OET by the remobilization of the uppermost sediments and its OM
- Small concentration of terrestrial OC (TOC < 0.5%) are preserved in seafloor sediments of deep-water domain